SEMI-ANNUAL STATUS REPORT

(9/1/75 to 2/29/76)

for

NASA Ames Research Grant No. NSG-2010

entitled

Three-Dimensional Dynamical and Chemical Modelling of the Upper Atmosphere

from

Ronald G. Prinn
(Principal Investigator)

Fred N. Alyea
(Co-Investigator)

Derek M. Cunnold
(Co-Investigator)

Department of Meteorology
Massachusetts Institute of Technology
Cambridge, Massachusetts 02139

Abstract

This report covers progress on NASA Grant NSG-2010 during the period September 1, 1975 to February 29, 1976. The coding of our 3-D upper atmospheric model for the ILIAC computer at NASA Ames Research Center is now nearing completion. Dr. Alyea presented a paper on the 3-D model at the Australian Conference on Climate and Climatic change held on December 7-11, 1975. Dr. Prinn attended the Space Shuttle Environmental Workshop on Stratospheric Effects in Houston, Texas on March 24-25, 1976 and reviewed our progress on modelling the ozone perturbations resulting from the Shuttle booster exhaust. Mr. Gary Moore, a graduate student, has been studying a time-dependent version of our 2-D model and is also investigating the sulfur cycle in the stratosphere. Drs Alyea, Cunnold and Prinn have recently been emphasizing the significant role of meteorology in influencing stratospheric composition measurements and in this regard Dr. Prinn presented a paper on this subject to the NASA Stratospheric Advisory Committee on Dec. 17, 1975 at NASA Goddard Space Flight Center. This paper will shortly appear in the Bulletin of the American Meteorological Society.

1. Introduction

We will discuss significant progress over the six-month period covered by this report under 3 main catagories: the 3-D model with full chemistry and its coding for the ILIAC IV, the impact of meteorology on measurement programs and measurement interpretation, and finally further work utilizing our 2-D model.

2. 3-D Chemical Dynamical Model

With the help of a full time programmer, the present 3-D model (with abbreviated chemistry) is being coded for the ILIAC IV computer and this arduous task is now nearing completion. We continue to use our CDI Teleterm 1030 terminal to aid this process. In the near future we should be ready to run a simple test version of the full dynamical program. The chemistry in the ILIAC IV version of our model will contain about 40 chemical reactions including those involving formation and removal of chlorine nitrate ($ClONO_2$). Our present full time programmer, M. Batish, will probably be replaced sometime this summer with a full time research scientist. We should have most of the programming complete by that time and be ready to run scientific experiments. We are presently considering suitable candidates with a good background in spectral modelling.

Dr. Alyea presented a paper on some of our 3-D modelling work at the "Australian Conference on Climate and Climatic Change" held in Clayton, Victoria, Australia on December 7-11, 1975. A copy of the paper entitled "Simulation experiments on the climate of the stratosphere and stratospheric ozone distributions under natural and man-made conditions" is appended to this report (Appendix I).

Dr. Prinn attended the "Space Shuttle Enviromental Workshop on Stratospheric Effects" held at the NASA Johnson Space Center on March 24-25, 1976. He gave a brief review there of our plans for simulating the ozone depletions resulting from the booster exhaust products. Some prelimimary runs of our 2-D model have been made and relevant results will appear in the workshop report. We do not have any de"inite numbers to report at this time and indeed we feel our best estimates will be made only after we have in operation the ILIAC version of our 3-D model with full chemistry.

3. Stratospheric Dynamics and Stratospheric Measurements

We have been particularly concerned over the past year with the problem posed by dynamically induced stratospheric variability and its influence on the planning and interpretation of measurements for minor constituents. Dr. Prinn presented a paper on this subject ot the NASA Stratospheric Advisory Committee Meeting held at the NASA Goddard Space Flight Center on 12/17/75. This paper entitled "The impact of stratospheric variability on measurement programs for minor constituents" is appended to this report (Appendix II). It has been accepted for publication in the Bulletin of the American Meteorological Society and will appear in the June, 1976 issue. We feel that a correct interpretation of stratospheric minor constituent measurements will entail careful use of 3-D modelling results and the known meteorological data for the observing sites. We also feel that observers should coordinate their observations in a much more meaningful manner than presently ex'sts. We are presently studying a few examples of recent fluorocarbon and ·Cl measurements in order to illustrate these ideas.

4. 2-D Chemical Model

Mr. Gary Moore, a graduate student, has recently completed a study of the effect of continuous time updating of transport parameters in 2-D models. He has written a detailed report entitled "A partial report on the time updating modifications made on the 2-D Stratospheric model, 2AM4" which will provide us with a useful reference for future use of this modelling approach. Mr. Moore has also been studying the cycle of sulfur in the atmosphere with particular emphasis on the production of stratospheric H_2SO_4 from the COS and SO_2 derived from fossil fuel combustion. He intends to ultimately model the stratospheric sulfuric acid layer utilizing our 2-D model but adding in the sulfur chemistry and modelling the important tropospheric removal mechanisms (rainout, washout, etc.) in some detail.

The impact of stratospheric variability on measurement programs for minor constituents[1]

Ronald G. Prinn

Fred N. Alyea

Derek M. Cunnold

Department of Meteorology

Massachusetts Institute of Technology

Cambridge, Massachusetts 02139

1. Presented at the NASA Stratospheric Advisory Committee Meeting, Dec. 17, 1975

(To appear in Bulletin Amer. Met. Soc., 1976)

ABSTRACT

The scales of temporal and spatial variations in stratospheric minor species concentrations and dynamical quantities are briefly reviewed. Despite the fact that the stratosphere is often considered as a very quiescent rogion of the atmosphere, it exhibits transient and generally unpredictable episodes of intense activity. The resultant necessity for some degree of coordination between different observers in their choice of locations and times for measurements of minor constituents is emphasized. We provide the specific suggestion of one or more short "International Stratospheric Periods" whose duration will depend upon the time of year. During these short periods as many observers as possible would perform an integrated series of observations designed to optimize the usefulness of their data to atmospheric scientists.

1. Introduction

Over the past few years, atmospheric scientists have become increasingly aware of the necessity and urgency for measurements of the concentrations of a significant number of stratospheric minor constituents. Of particular concern has been the need for a sound observational basis for evaluating the stratospheric ozone models that have recently been used for predictions of ozone depletion by anthropogenic trace gases such as NO and NO_2 from supersonic aircraft, and $CFCl_3$ and CF_2Cl_2 from aerosol cans and refrigerators. Considerable effort has been taken to delineate those species and dynamical variables whose measurement will contribute most to these model validations. In contrast, the possible need for a significant degree of coordination between different observers in their choice of times and locations for these measurements has received comparatively little attention.

For species with chemical time constants which appear to be smaller than typical advection times, there are a number of persuasive arguments for considering simultaneous measurements as discussed at a recent workshop on the stratosphere (NASA, 1975). A few of such types of observations in fact already exist (Ackerman et al, 1975; Lowenstein and Savage, 1975; Evans et al, 1975). Examples of groups of species for which simultaneous measurements are highly desirable are: odd nitrogen (NO, NO_2, HNO_3), odd oxygen (O, O_3), chlorine (Cl, ClO, HCl), and odd hydrogen (OH, HO_2, H_2O_2). Since many of these short-lived species are predicted to exhibit significant variations with time of day (Whitten and Turco, 1974) and with latitude and season (Prinn et al, 1975), the hour and location of such observations is clearly an important ingredient in their interpretation. Fortunately most observers appear fully aware of such considerations so we need not pursue these requirements any further here.

However, somewhat less emphasis has been given to the coordination of measurements involving species whose concentrations depend on both chemical and advective processes. Utilizing observations and numerical model results we can readily show that the temporal and spatial variability of such minor species is significant. In addition, we know there exist important variations in stratospheric temperature (which will influence the chemical terms) and stratospheric motions (which will govern the advective terms). Such inhomogeneities should obviously be fully appreciated in planning observational programs.

2. Dynamical variability

Let us begin by looking at a few examples of the oscillations in dynamical variables in the stratosphere. In doing so we will tend to choose cases which will illustrate the greatest variability. This should not be interpreted as an attempt to overstate our case but rather as providing a review of the significant changes which can occasionally occur in the stratosphere.

Rapid alterations in stratospheric temperature are of course well known to meteorologists. The most impressive are the Sudden Stratospheric Warmings and in Fig. 1 we show the temperature changes observed over Scotland (57°N) during the 1967-68 warming (Quiroz, 1971). Of particular interest to our discussion here is the fact that the temperature increased by 80°C over a ten-day period at the 43 km level. This particular warming was indeed strong enough to cause the usual winter circumpolar vortex (westerlies) to be replaced temporarily with anticyclonic easterlies. Such impressive events appear to occur about once every one or two years.

Warmings on a smaller scale occur with greater frequency and in a generally unpredictable manner. The magnitude and frequency of these minor warmings is particularly well illustrated in Fig. 2 in which temperatures at the 30 mb level at high and mid-latitudes are given for two winter seasons (Madden, 1975). The observed temperature oscillations typically exhibit 1-3 week periods. The 1967-68 major warming is also clearly illustrated. In recent unpublished runs of our 3-dimensional stratospheric circulation model at M.I.T. (see Cunnold et al, 1975), we have also obtained many minor winter warming events and these are shown as functions of longitude and time at 45 km in Fig. 3. In addition to the general warming at 45 km the reader should note what appears to be a Rossby wave with zonal wave number 1 travelling westward at ~ 3 m sec^{-1}. This produces temperature oscillations $\sim 50°K$ in addition to the general warming. At 30 km specific wave numbers are less obvious but significant temperature oscillations are present there also. As a further example, northern hemisphere temperature changes observed over a 7-day period in March, 1964 are shown in Fig. 4 (Newell et al, 1974). Alterations in vertical velocities deduced using the thermodynamic equation are also depicted in the latter illustration.

The standard deviations for the stratospheric meridional wind during the winter imply typical variations ranging up to 25 m sec^{-1}. Standard deviations during the summer are usually about a factor of 3 or 4 less (Newell et al, 1966). The daily variation of the zonal wind during March, 1964 is shown in Fig. 5 (Dopplick, 1971). At 30 km altitude, 15 m sec^{-1} westerly winds reverse to 15 m sec^{-1} easterlies in a period of about 2 weeks. For estimating daily variations in advective terms we are of course concerned with daily correlations between the wind field components and the various transported quantities. The variability of the northward eddy flux of heat at 60°N can be equated with the substantial oscillations in the convergence of this heat flux northward of 60°N which are shown in Fig. 2. As a further example, the daily variation of the vertical eddy flux of geopotential is given in Fig. 6 for February, 1964 (Dopplick, 1971). The substantial variations in this energy flux with both latitude and time should be particularly noted. We will give further examples of the daily variability of such correlations shortly.

Transport processes across the tropopause are also of particular concern for quantitative studies of upper atmospheric trace constituents. Reiter (1975) estimates that during one year about 40% of the total stratospheric air mass is exchanged with the troposphere through the tropical Hadley cell, 20% through large-scale eddy transports in the jet stream region, and 10% through seasonal changes in tropopause heights. The upward flux in the tropical branch of the Hadley cell mainly occurs through localized and transient cumulus convection (Riehl and Malkus, 1958), while exchange of air in the jet stream region can be related to tropospheric cyclonic activity (Mahlman, 1965). Thus these two processes are expected to have significant temporal and spatial variations. In Fig. 7 we illustrate the surprisingly large variability in the January, 1973 tropopause position (Reiter, 1975). The July, 1973 variability is somewhat smaller but nevertheless still significant. This has implications both for tropospheric-stratospheric exchange and for variations in the dynamical stability (eg. Richardson number) in the 100 – 500 mb region.

The differences between January and July just noted remind us we should also discuss scales of variability during different seasons. Both theory and observation (see Holton, 1975 for a review) suggest that vertically-propagating extra-tropical planetary waves provide the major energy source for driving the lower stratosphere. This upward flux is modulated in part by downward reflection of quasi-stationary Rossby waves by easterly winds in summer and strong westerly winds in winter (Charney and Drazin, 1961). This modulation is evident in Fig. 8 where we have shown the daily vertical eddy flux of geopotential through the 100 and 10 mb levels during 1964 (Dopplick, 1971). Similar annual cycles in the variance of temperature and meridional wind are evident at most stratospheric levels in unpublished data here at M.I.T. We therefore expect the most rapid and largest variations in dynamical variables during the late winter months and indeed most of the examples we have just provided are derived from this period. Of particular importance for our discussion here, is the time-scale over which we may expect no significant dynamical changes and this is clearly very different in summer and winter seasons.

3. Minor constituent variability

Having thus noted the dynamical variabilty of stratospheric air, we can move on to discuss similar effects for stratospheric minor constituents whose local concentrations are affected by the scales and velocities of mixing processes as well as chemistry. Although the majority of the important longer-lived stratospheric species have not been measured at a wide range of localities and over extended periods of time, enough data does exist (eg. for O_3, H_2O, HNO_3, H_2SO_4, CCl_3F, and SF_6) to illustrate the types of inhomogeneities we should expect in stratospheric air. As we implied earlier, our principal thesis will be that uncoordinated observations of different species at different localities and/or times are in general incompatible. As a result erroneous estimates of vertical profiles may result from simple superposition of such uncoordinated measurements.

Let us look at some typical early spring ozone variations. In Fig. 9 we illustrate the temporal and latitudinal variations in total ozone observed during March, 1964 (Newell et al, 1973). It is clear that total ozone increases of up to 50% may occur at mid-latitudes over a time span as short as ten days. The quasi-horizontal eddy activity shown in Fig. 9 is also increasing very significantly during this particular period. Observations at the same latitude but 10 days apart would therefore provide significantly different results. Similar rapid temporal variations occur in ozone concentrations at various altitudes as illustrated over Switzerland in Fig. 10 (Dütsch, 1974). In the latter case we see that factor of 8 changes over a period of ~3 days are not unusual. Significant variations in total ozone ($\lesssim$ 25%) also occur with longitude (Reiter and Lovill, 1974) as illustrated in Fig. 11 for 20°N latitude. Most readers will be familiar with the significant variations in monthly mean total ozone as a function of position and season (Dütsch, 1971) and such variations have been simulated in the M.I.T. model (Alyea et al, 1975).

Unfortunately, measurements of water vapor in the stratosphere are few and generally restricted to Europe and North America. Spatial and temporal variabilities are certainly expected because of temperature changes and the localized and transient injections of water vapor into the lower stratosphere associated with the tropical upwelling (ie. cumulus towers) and with mid-latitude thunderstorms. We can illustrate our case using recent observations of the latitudinal dependence of the H_2O mixing ratio in the 15 - 20 km region during October, 1973 through January, 1974 which are illustrated in Fig. 12 (Kuhn et al, 1975). Note the doubling of this ratio in the region of the ITCZ.

Observations of hydrogen nitrate and sulfuric acid have exhibited significant altitude and latitude variations. A summary of global observations during Northern Hemisphere Spring by Lazrus and Gandrud (1974) is given in Fig. 13 and the HNO_3 observations can be compared with our 2-D model results (Prinn et al, 1975) which show qualitative agreement with these data. The HNO_3 map is constructed by superimposing various observations during the Spring of 1971 and agreement with a 2-D model in which short-term variations are essentially averaged out is perhaps not surprising. The process of superposition is of course contradictory to the general theme of this paper but our purpose in presenting such results is to qualitatively illustrate the spatial variability of HNO_3. Significant spatial variations suggest that significant temporal variations will result during sporadic rapid large-scale interchange of air parcels of the type discussed earlier. The fact that lower stratospheric mixing appears to be dominated by large-scale rather than very small scale motions (Cunnold et al, 1975; Heck and Panofsy, 1975) reinforces this notion.

As a final example we show in Fig. 14 the observed latitudinal variations in CCl_3F during April and October, 1974 (Krey and Lagomarsino, 1975). Variations are most significant in the vertical and temporal variations over at least a 6 month period cannot be neglected. Similar results were obtained by these workers for SF_6.

4. An International Stratospheric Period

It is hoped that we have provided a sufficient case for concern over the inhomogeneity of the stratosphere. We particularly emphasize that superposition of profiles of different species measured at different positions and times is in general hazardous. In addition, we must be prepared to accurately scale localized vertical profile observations to the annual global average for comparison with 1-D models in which most of the ozone predictions have been made. Multi-dimensional models, particularly 3-D models where dynamics are predicted, will play an important role here but we are still faced with the problem of day to day predictability of the stratosphere. We must therefore obtain some idea of temporal variations on a monthly or seasonal scale. These observations need not be continuous in space and time providing imaginative use of 3-D numerical models and existing stratospheric observations is made.

With these points in mind we would like to recommend the designation of one or more "International Stratospheric Periods" (ISP) for the purpose of coordinating existing measurement projects. In each ISP we suggest the following scenario for the timing and location of observations and their interpretation:

1) Each ISP should be defined with enough lead time being provided to observers to prepare for participation. The existing funding agencies in North America, and if possible in Europe and Australasia, should encourage their various observing groups to cooperate fully during these periods.

2) The duration of each ISP will vary with the time of year chosen. Based on our earlier discussion we suggest intervals of about 1-3 days

during late Fall, Winter, and early Spring; about 1 week during early Fall and late Spring; and about 2 weeks during Summer. If one ISP is planned each year then a different season could be chosen each time.

3) Balloon and rocket flights during ISP should be as far as possible chosen so as to ensure measurements of vertical profiles of as many constituents and dynamical variables as possible above each station. In the event that this is not possible, superposition of the results from different stations at the same latitude and local time of day is generally preferable to superposition of results from stations of the same longitude. The aim would be to obtain self-consistent sets of vertical profiles for at least one high-latitude, one mid-latitude and one low-latitude station. Southern hemisphere coverage would initially be sparse but would hopefully improve in later years.

4) Aircraft flights and satellite observations during ISP should cover the regions above and between the stations in 3). This will provide knowledge of horizontal variations and help to relate the localized measurements at each station to the global picture at the time of ISP. Some coverage of the Southern hemisphere would also be useful for assessing the global picture.

5) As soon as possible after the ISP all the results should be compiled into a compact data report made readily available to the atmospheric scientific community. This report would be recognized as preliminary; it would not preclude subsequent publication of both the data and methods in the open literature. Recognizing the forcing role of the troposphere, this volume should also include pertinent global tropospheric and lower stratospheric meteorological data obtained during the ISP under existing daily atmospheric observation programs.

5. Concluding remarks

We feel that a scenario of the type proposed here will considerably increase the usefulness of future stratospheric measurements for aeronomers and meteorologists alike. To conclude, we should emphasize that except for funding of a small staff for coordination and data report compilation purposes, there is no requirement for additional funding over and above that provided by existing agencies. There should be no hint of a central controlling agency; each observer would have to obtain his own funds based on the merits of his particular experiment. We also recognize that the vagaries of instrument development and the weather may prevent participation by some observers during a particular ISP. However, even partial success in such a venture must be deemed superior to allowing a haphazard and totally uncoordinated program for measurement of stratospheric minor constituents to exist.

References

Ackerman, J., D. Fontanella, D. Frimont, A. Girard, N. Louisnard, and C. Muller, 1975: Simultaneous measurements of NO and NO_2 in the stratosphere, Planetary Space Sci. 23, 651-656.

Alyea, F., D. Cunnold, and R. Prinn, 1975: Stratospheric ozone destruction by aircraft-induced nitrogen oxides, Science 188, 117-121.

Charney, J. and P. Drazin, 1961: Propagation of planetary-scale distributions from the lower into the upper atmosphere, J. Geophys. Res. 66, 83-109.

Cunnold, D., F. Alyea, N. Phillips, and R. Prinn, 1975: A three dimensional dynamical-chemical model of atmospheric ozone, J. Atmos. Sci. 32, 170-194.

Dopplick, T. G., 1971: The energetics of the lower stratosphere including radiative effects, Quart. J. Roy. Met. Soc. 97, 209-237.

Dütsch, H., 1971: Photochemistry of atmospheric ozone, Advan. in Geophys. 15, 219-322.

Dütsch, H., 1974: Regular ozone soundings at the aerological station of the Swiss meteorological office at Payern, Switzerland, 1968-1972, Lapeth - 10, Laboratory for Atmospheric Physics ETH, Zurich, Switzerland.

Evans, W., J. Kerr, and D. Wardle, 1975: The AES Stratospheric balloon measurements project: preliminary results, Internal Report No. APRB 30 X 2, Atmospheric Environment Service, Downsview, Ontario, Canada.

Heck, W. and H. Panofsky, 1975: Paper presented at the IUGG 16th General Assembly, Grenoble, France.

Holton, J. R., 1975: The dynamic meteorology of the stratosphere and mesosphere, American Meteorological Society, Boston, Mass.

Krey, P., and R. Lagomarsino, 1975: Stratospheric Concentrations of SF_6 and CCl_3F, Preprint, Health and Safety Lab., ERDA, New York, N.Y.

Kuhn, P., L. Stearns, and M. Lojko, 1975: Latitudinal profiles of stratospheric water vapor, Geophys. Res. Lett. 2, 227-230.

Lazrus, A. L. and B. W. Gandrud, 1974: Distribution of Stratospheric Nitric Acid Vapor, J. Atmo. Sci. 31, 1102-1108.

Lowenstein, M. and H. Savage, 1975: Latitudinal measurements of NO and O_3 in the lower stratosphere from 5° to 80° North, Geophys. Res. Lett. 2, 448-450.

Madden, R. A., 1975: Oscillations in the winter stratosphere: Part 2. The role of horizontal eddy heat transport and the interaction of transient and stationary planetary-scale waves. Mon. Wea. Rev. 103, 717-729.

Mahlman, J. D., 1965: Relation of upper air hemispheric index patterns to seasonal fallout fluctuations, AEC Symp. Ser. 5, 4664-476.

NASA, 1975: The Stratosphere, 1975-1980. D. Hunten, editor, Goddard Space Flight Center, Greenbelt, Maryland.

Newell, R., J. Wallace, and J. Mahoney, 1966: The general circulation of the atmosphere and its effects on the movements of trace substances, Tellus 18, 363-380.

Newell, R., G. Boer, and T. Dopplick, 1973: Influence of the vertical motion field on ozone concentration in the stratosphere, Pure Appl. Geophys. 106-108, 1531-1543.

Newell, R., G. Herman, J. Fullmer, W. Tahnk, and M. Tanaka, 1974: Diagnostic studies of the general circulation of the stratosphere, Rep. No. COO-2195-11, Dept. of Meteorology, MIT, Cambridge, Mass.

Prinn, R., F. Alyea, and D. Cunnold, 1975: Stratospheric distributions of odd nitrogen and odd hydrogen in a two-dimensional model, J. Geophys. Res. 80, 4997-5004.

Quiroz, R. S., 1971: The determination of the amplitude and altitude of stratospheric warmings from satellite-measured radiance changes, J. Applied Met. 10, 555-574.

Reiter, E. R., 1975: Stratospheric-tropospheric exchange processes, Rev. Geophys. Space Phys. 13, 459-474.

Reiter, E. and J. Lovill, 1974: The longitudinal movement of stratospheric ozone waves as determined by satellite, Arch. Meteorol. Geophys. Bioklimatol. A23, 13-27.

Riehl, H., and J. Malkus, 1958: On the heat balance of the equatorial trough zone, Geophysica 6, 505-538.

Whitten, R., and R. Turco, 1974: Diurnal variations of HO_x and NO_x in the stratosphere, J. Geophys. Res. 79, 1302-1304.

Figure Captions

1. Stratospheric temperatures T (°C) observed over West Geirinish, Scotland (57°N) at various altitudes (km) during and after the December, 1967 Sudden Stratospheric Warming (after Quiroz, 1971).

2. Zonal mean temperatures T (°C) for 70-80°N (HIGH LATITUDES) and 40-50°N (MIDDLE LATITUDES) during the winters of 1967-1968 (upper) and 1971-1972 (lower). Also illustrated is the convergence of the meridional eddy heat flux (°C/day) northward of 60°N (EDDY CONV). The latter flux is defined as the zonally-averaged correlation between the geostrophic perturbation meridional velocity v* (m sec^{-1}) and the perturbation temperature T* (°C), with only the first six zonal wave numbers being considered. All data refer to the 30 mb level.

3. Stratospheric temperatures T (°C) obtained during January and February at 70°N from a run of the MIT Stratospheric Circulation Model. Data are given for the 2 mb level.

4. Northern hemisphere stratospheric temperature T (°C) observed at the 10 mb level on March 19 and 12 during the 1964 spring warming (solid lines). Also shown (dashed lines) are vertical velocities ω (10^{-5} mb sec^{-1}) computed from observations for the same period using the thermodynamic equation (after Newell et al, 1974).

5. Daily longitudinally-averaged zonal winds u (m sec^{-1}) at the 10 mb level computed from Northern hemisphere observations assuming geostrophy for March, 1964 (after Dopplick, 1971).

6. Daily zonally-averaged correlations in the Northern Hemisphere between vertical perturbation velocity in the Northern Hemisphere ω^* (10^{-5} mb sec^{-1}) and perturbation geopotential height Z^* (cm) at the 10 mb level during February, 1964 (after Dopplick, 1971). This correlation has the units of energy flux (deciwatt m^{-2}) and constitutes the pressure work contribution to the total vertical wave energy flux. A negative correlation denotes an upward flux.

7. Cumulative percent frequency distribution of tropopause pressures over North America during January, 1963 (after Reiter, 1975).

8. Daily horizontally-averaged correlations in the Northern hemisphere between ω^* (10^{-3} mb sec^{-1}) and Z^* (cm) at the 10 and 100 mb levels during 1964 (after Dopplick, 1971). The units are deciwatt m^{-2} (see Fig. 5 for physical interpretation).

9. Total columnar ozone (cm. mb) and zonally averaged correlation between ω^* (mb sec^{-1}) and v^* (m sec^{-1}) at the 100 mb level during 1964 Northern hemisphere March. The latter correlation is positive for northward and downward (ie. quasi-horizontal) eddy transport (after Newell, et al, 1973).

10. Ozone partial pressures (10^{-6} mb) and atmospheric temperatures (°C) observed as functions of pressure (mb) over Payerne, Switzerland on February 20 (solid lines) and 23 (dashed lines), 1970. Lines of constant ozone mass mixing ratio (10^{-6} gm O_3 per gm air) are also shown (after Dutsch, 1974).

11. Total columnar ozone (cm. mb) observed at 20°N during June 1969 by the NIMBUS III IRIS experiment (after Reiter and Lovill, 1974).

12. Average water vapor mixing ratios (10^{-6} gm H_2O per gm air) observed in the 15–20 km altitude region during the period October, 1973 through January, 1974 (after Kuhn et al, 1975).

13. Aircraft observations at various altitudes (km) of the mass mixing ratios (10^{-9} gm per gm air) of HNO_3 gas (lower graph) and sulfuric acid aerosol (upper graph) during the 1971 Northern hemisphere Spring and Southern hemisphere Fall (after Lazrus and Gandrud, 1974).

14. Volume mixing ratios (part per 10^{12}) of the chlorofluorocarbon CCl_3F observed at various altitudes (km) during April (left hand side) and October (right hand side), 1974 (after Krey and Lagomarsino, 1975). The tropopause position is indicated by a dashed line.

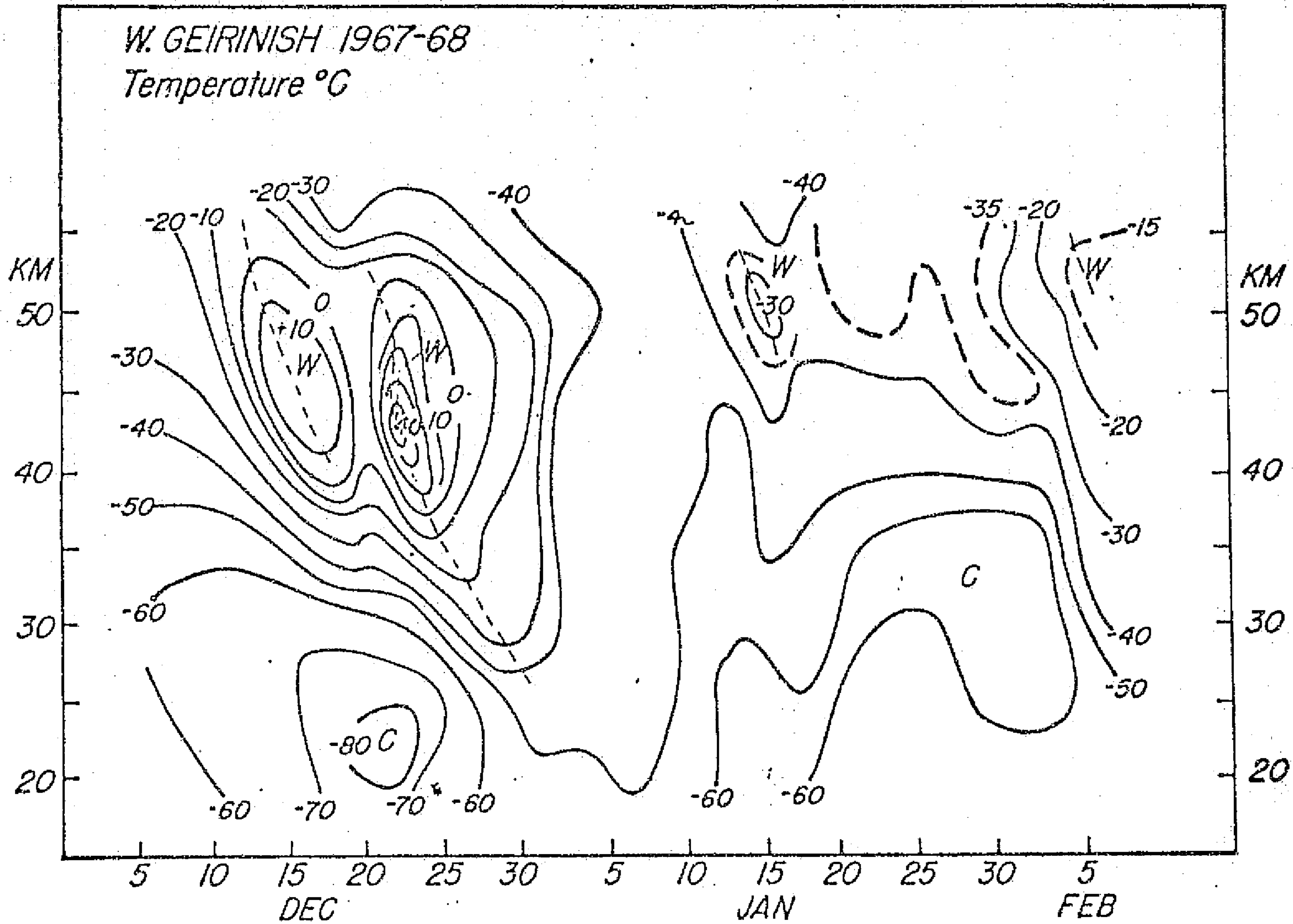

REPRODUCIBILITY OF THE ORIGINAL PAGE IS POOR

Figure 1

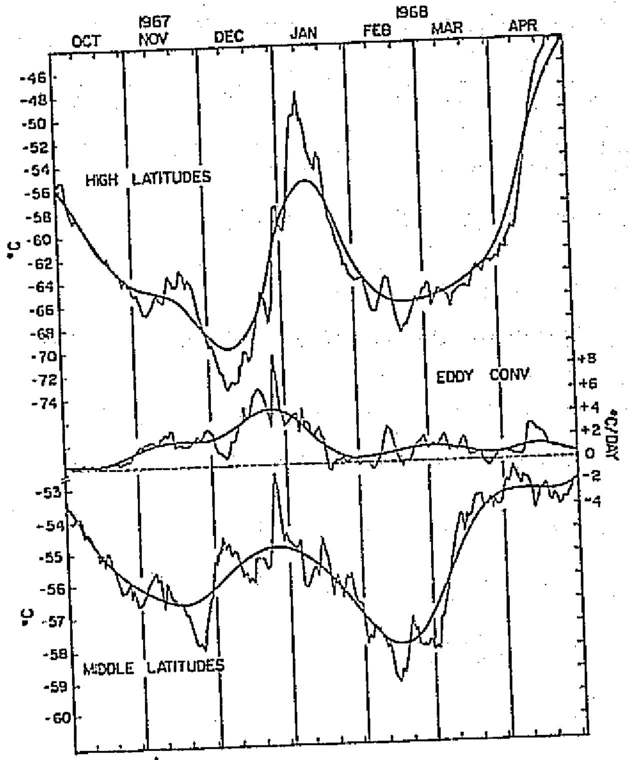
1967
1968
OCT
NOV
DEC
JAN
FEB
MAR
APR
HIGH LATITUDES
EDDY CONV
MIDDLE LATITUDES
°C
°C/DAY

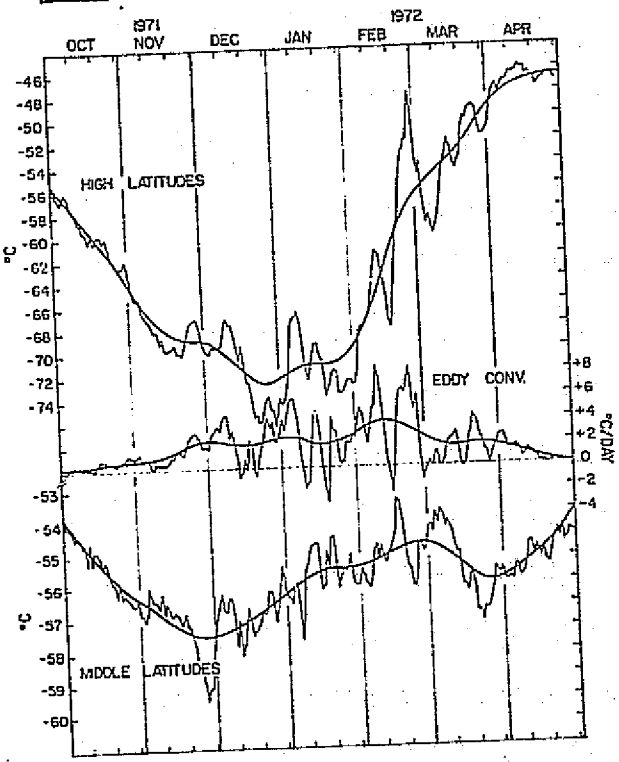
1971
1972
OCT
NOV
DEC
JAN
FEB
MAR
APR
HIGH LATITUDES
EDDY CONV.
MIDDLE LATITUDES
°C
°C/DAY

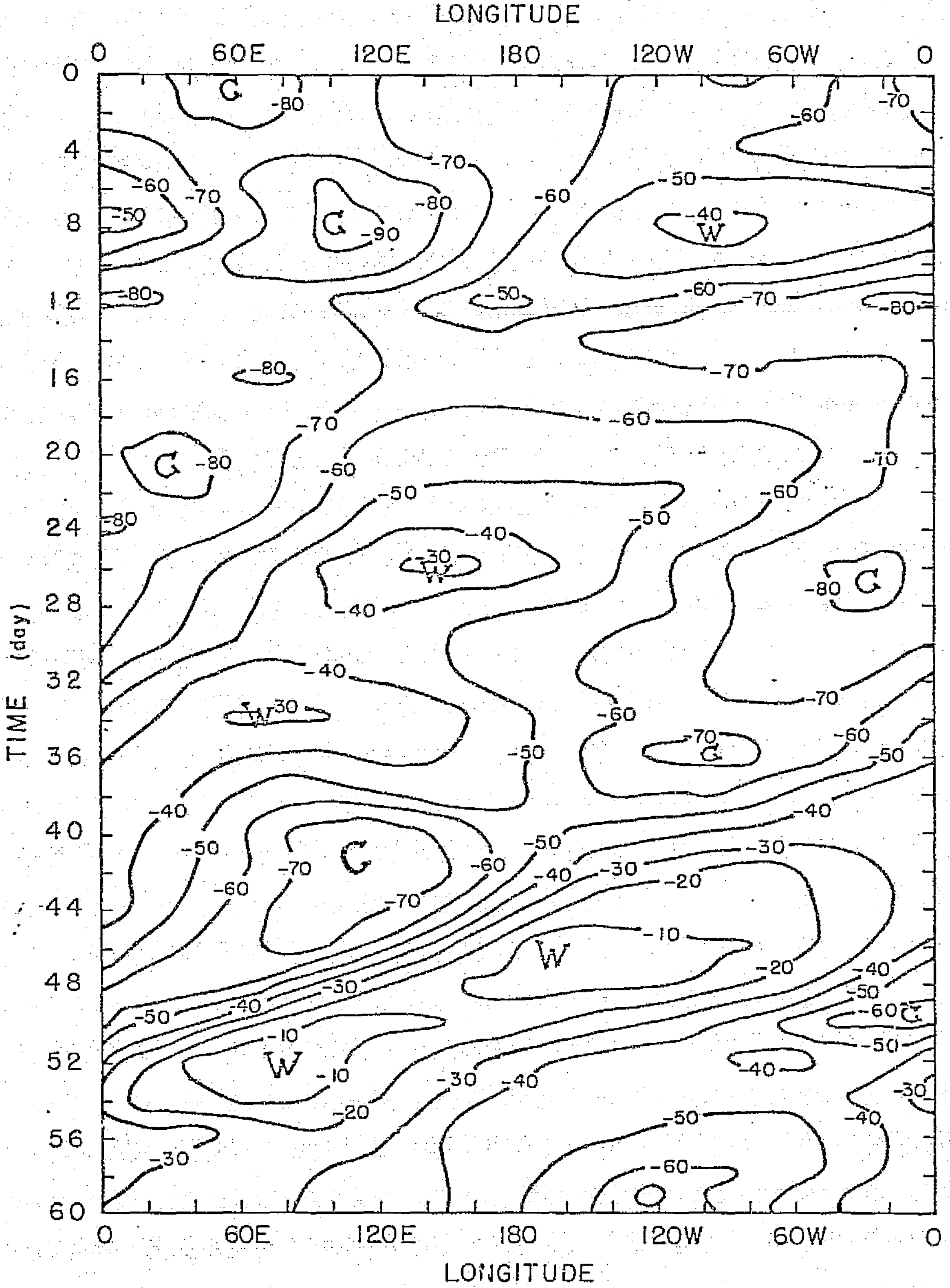

RUN 21: TEMPERATURE (°C) : LONGITUDE VS TIME
70° N. LATITUDE, ~ 45 km (2 mb)

Figure 3

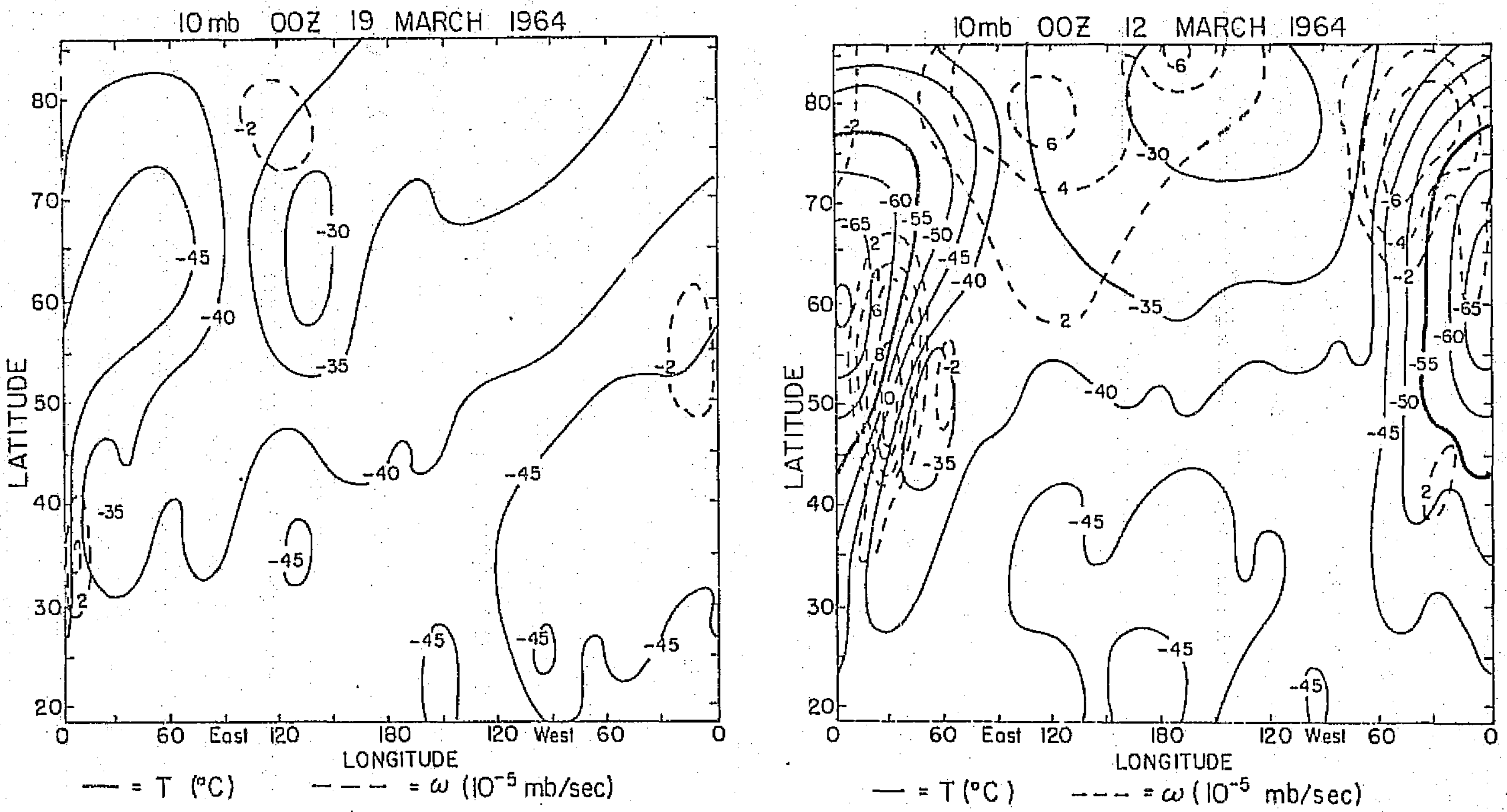
10 mb 00Z 19 MARCH 1964
LATITUDE
LONGITUDE
East
West
— = T (°C) - - - = ω (10⁻⁵ mb/sec)
10 mb 00Z 12 MARCH 1964
LATITUDE
LONGITUDE
East
West
— = T (°C) - - - = ω (10⁻⁵ mb/sec)

Figure 4

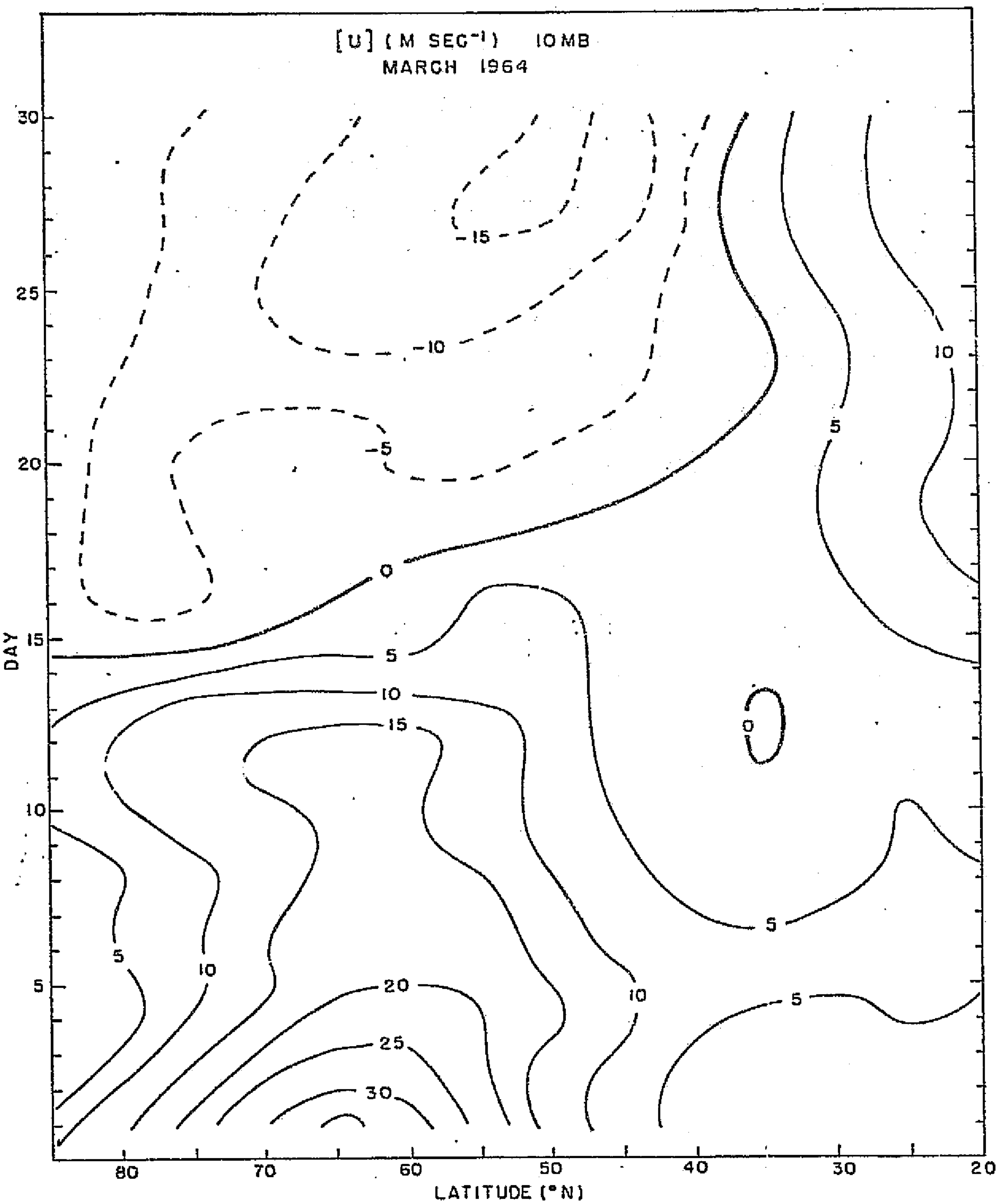
[U] (M SEC⁻¹) 10 MB
MARCH 1964
DAY
LATITUDE (°N)
30
25
20
15
10
5
80
70
60
50
40
30
20
-15
-10
-5
0
5
10
15
20
25
30

Figure 5

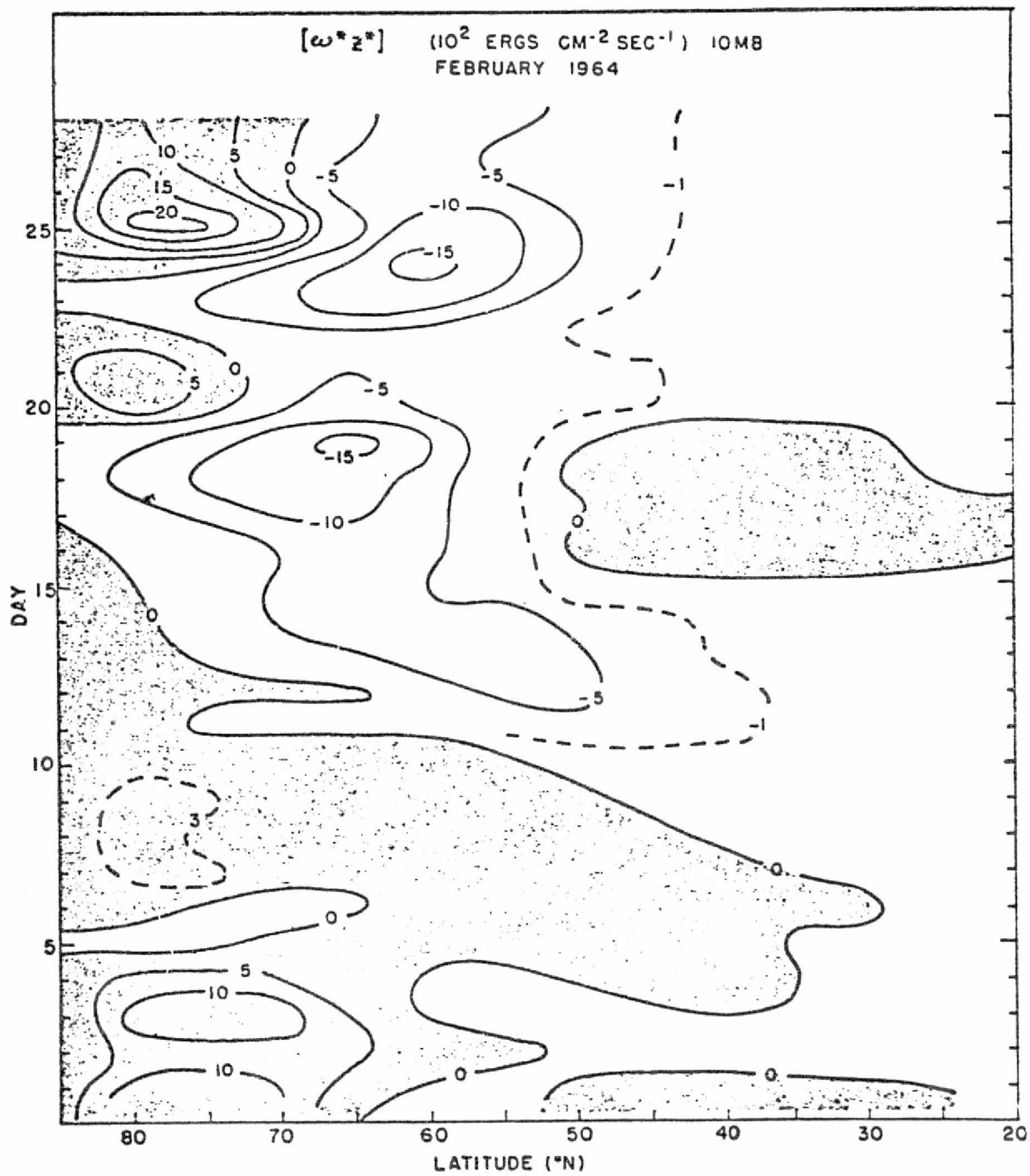

[ω* z*] (10² ERGS CM⁻² SEC⁻¹) 10MB
FEBRUARY 1964
DAY
LATITUDE (°N)
80
70
60
50
40
30
20
5
10
15
20
25

Figure 6

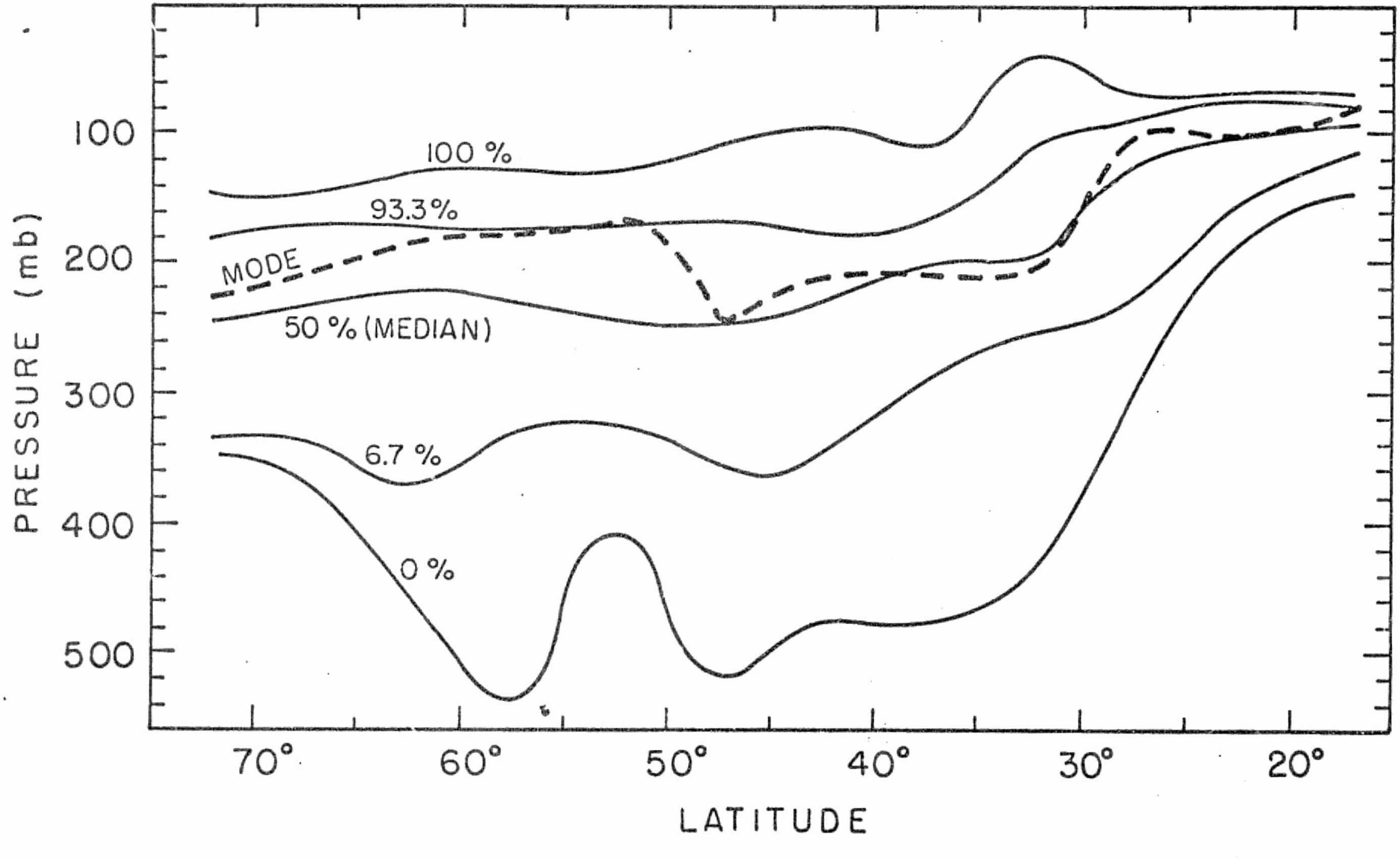

PRESSURE (mb)
100
200
300
400
500
100 %
93.3%
MODE
50 % (MEDIAN)
6.7 %
0 %
70°
60°
50°
40°
30°
20°
LATITUDE

Figure 7

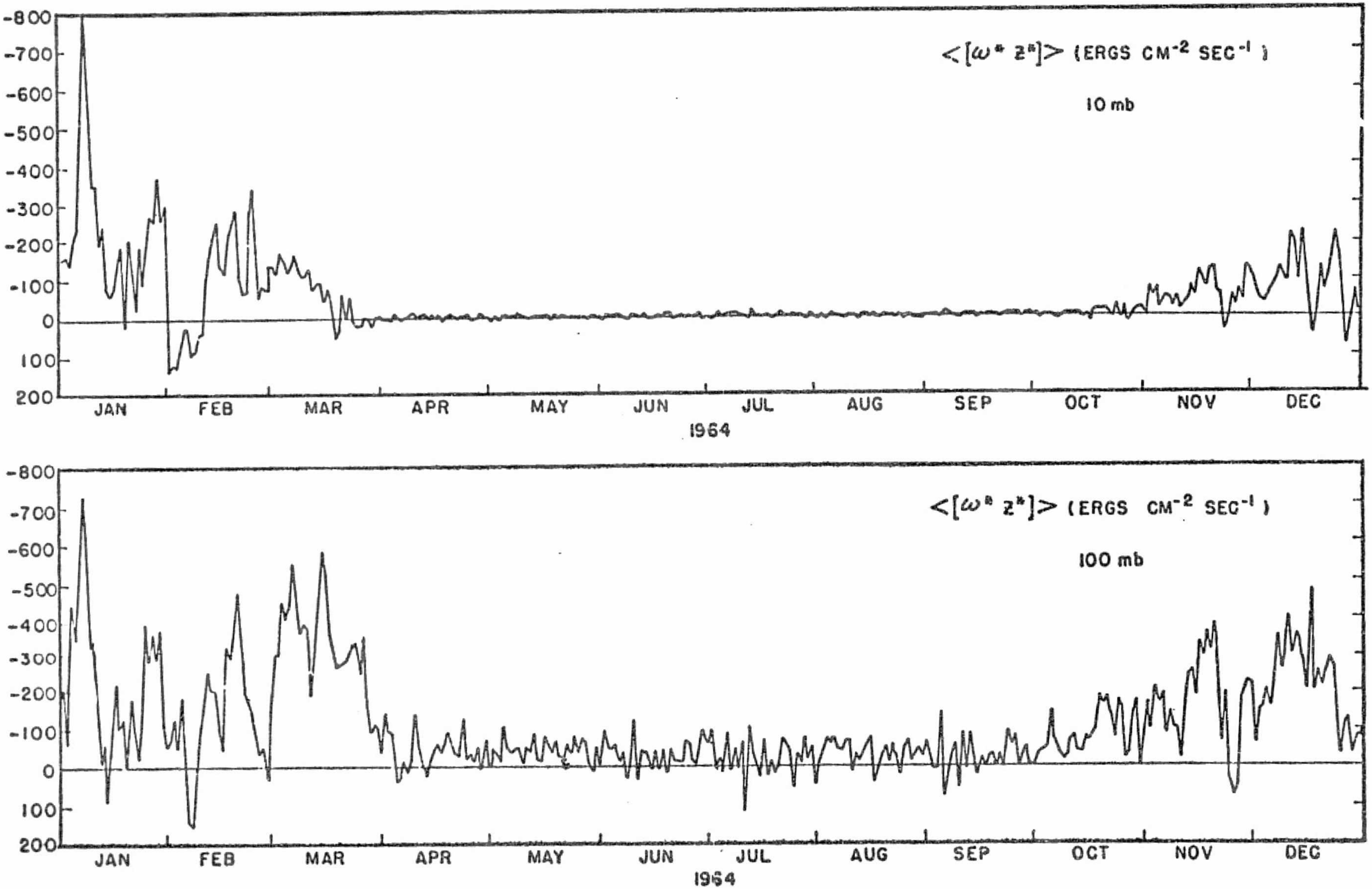
<[ω* z*]> (ERGS CM-2 SEC-1)
10 mb
-800
-700
-600
-500
-400
-300
-200
-100
0
100
200
JAN FEB MAR APR MAY JUN JUL AUG SEP OCT NOV DEC
1964
<[ω* z*]> (ERGS CM-2 SEC-1)
100 mb
-800
-700
-600
-500
-400
-300
-200
-100
0
100
200
JAN FEB MAR APR MAY JUN JUL AUG SEP OCT NOV DEC
1964

Figure 8

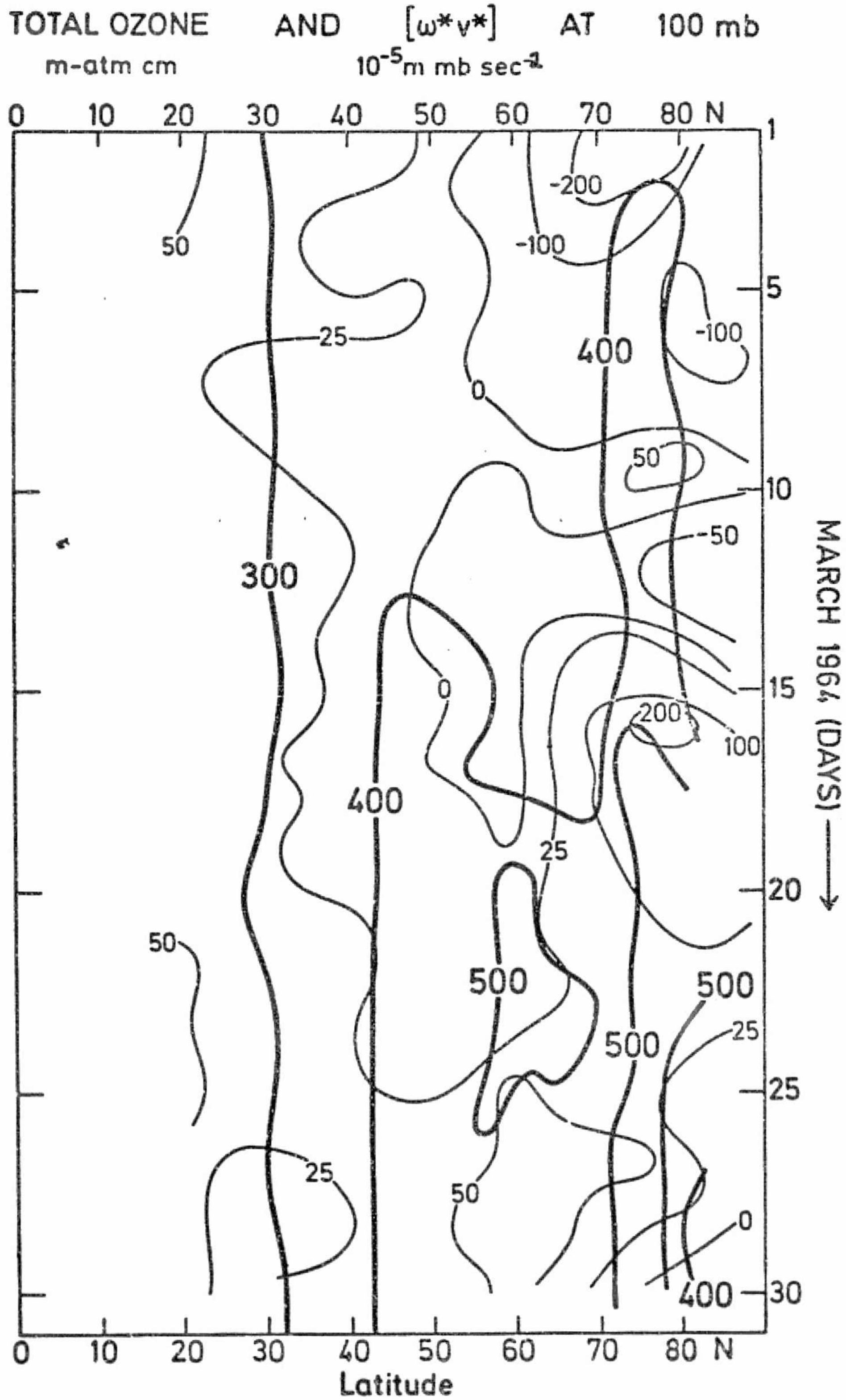
TOTAL OZONE AND [ω*v*] AT 100 mb
m-atm cm
10^-5 m mb sec^-1
0 10 20 30 40 50 60 70 80 N
1
5
10
15
20
25
30
MARCH 1964 (DAYS)
-200
-100
50
25
400
0
300
-50
200
100
500
Latitude

Figure 9

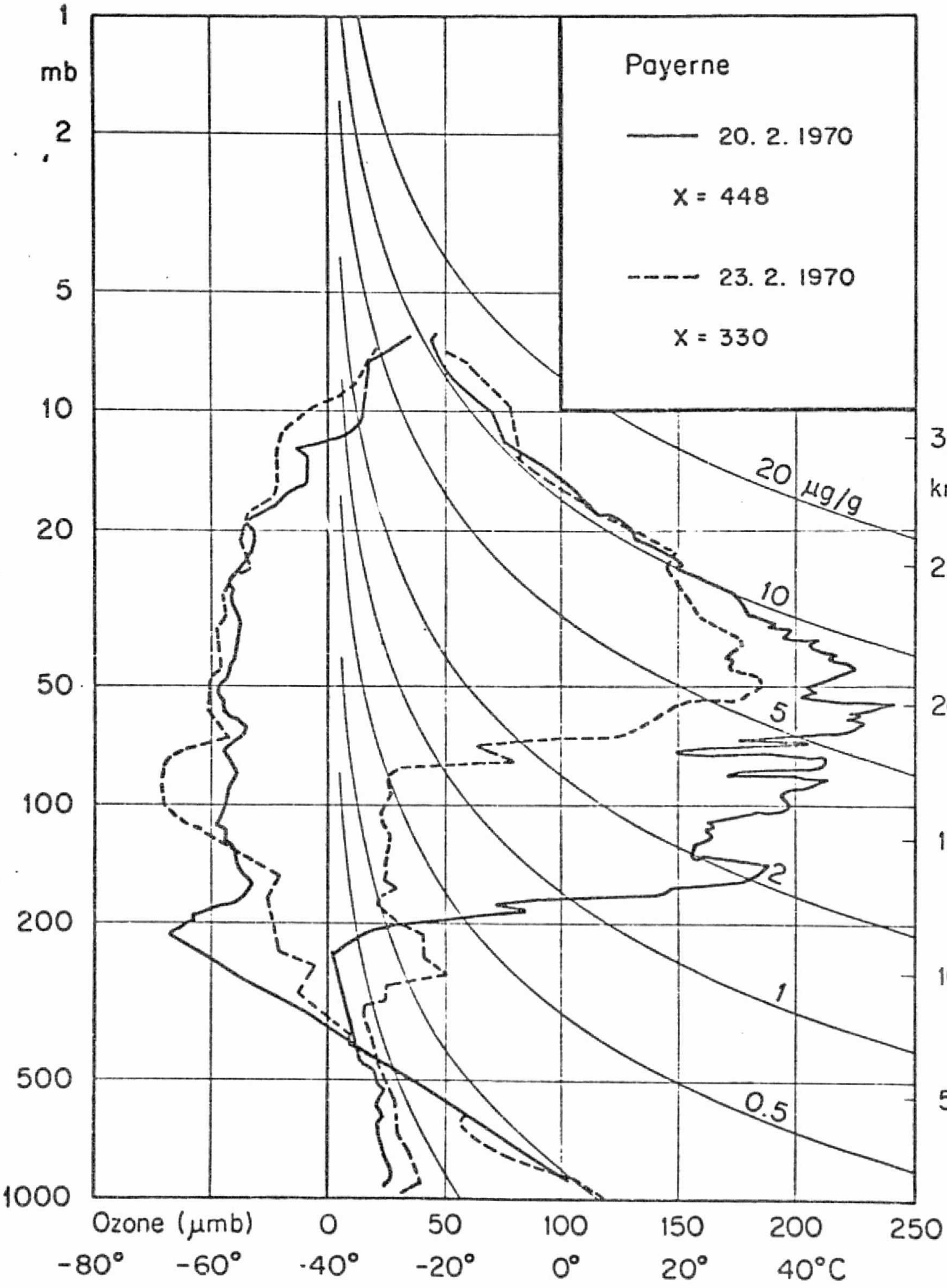
1
mb
2
5
10
20
50
100
200
500
1000
Payerne
20. 2. 1970
X = 448
23. 2. 1970
X = 330
30
km
25
20
15
10
5
20 µg/g
10
5
2
1
0.5
Ozone (µmb)
0
50
100
150
200
250
-80°
-60°
-40°
-20°
0°
20°
40°C

Figure 10

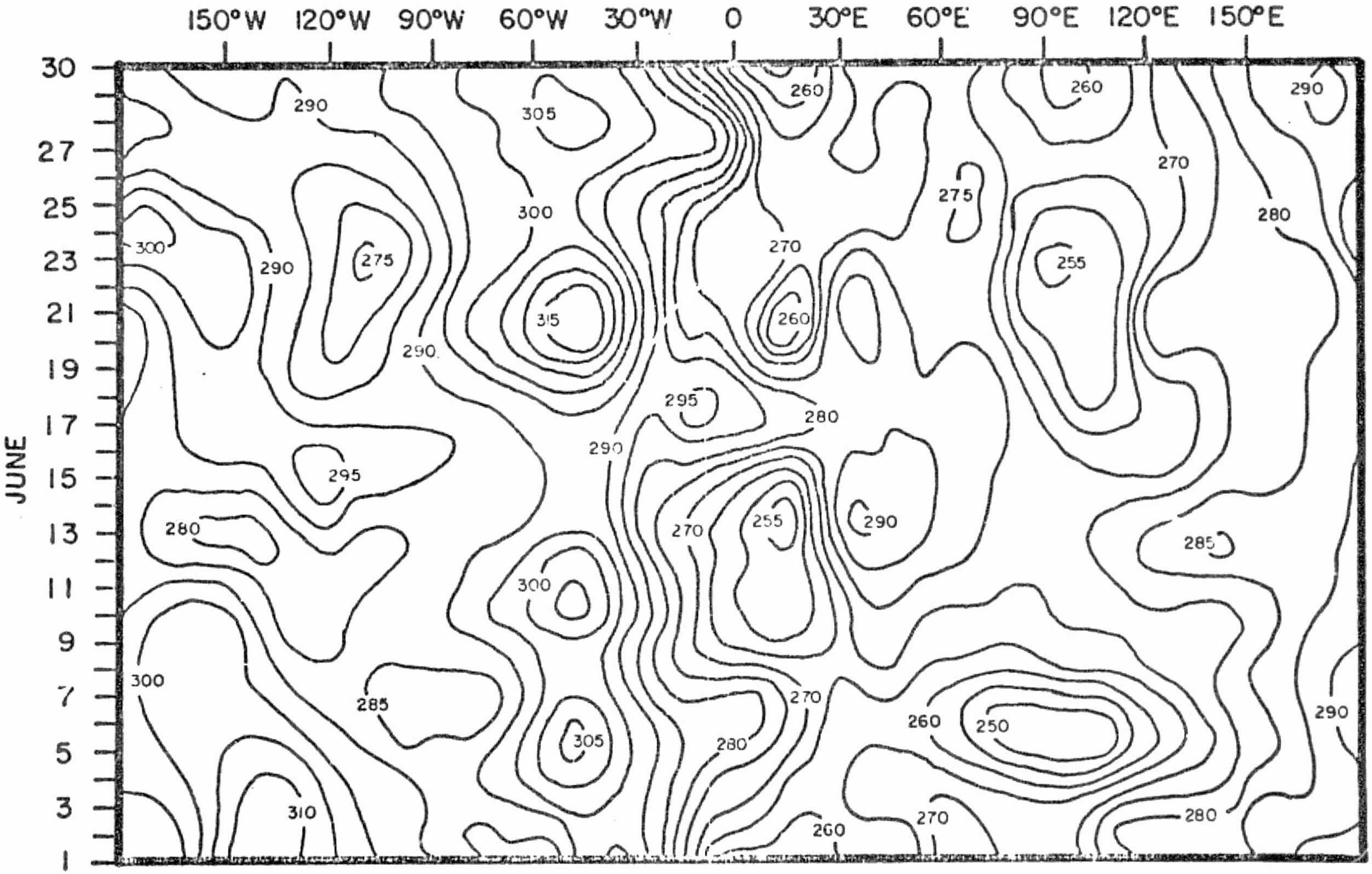
150°W 120°W 90°W 60°W 30°W 0 30°E 60°E 90°E 120°E 150°E
JUNE
30
27
25
23
21
19
17
15
13
11
9
7
5
3
1
290
305
260
260
290
270
275
300
280
300
290
275
270
255
315
260
290
295
280
290
295
280
255
290
270
285
300
300
285
305
270
260
250
290
280
310
260
270
280

Figure 11

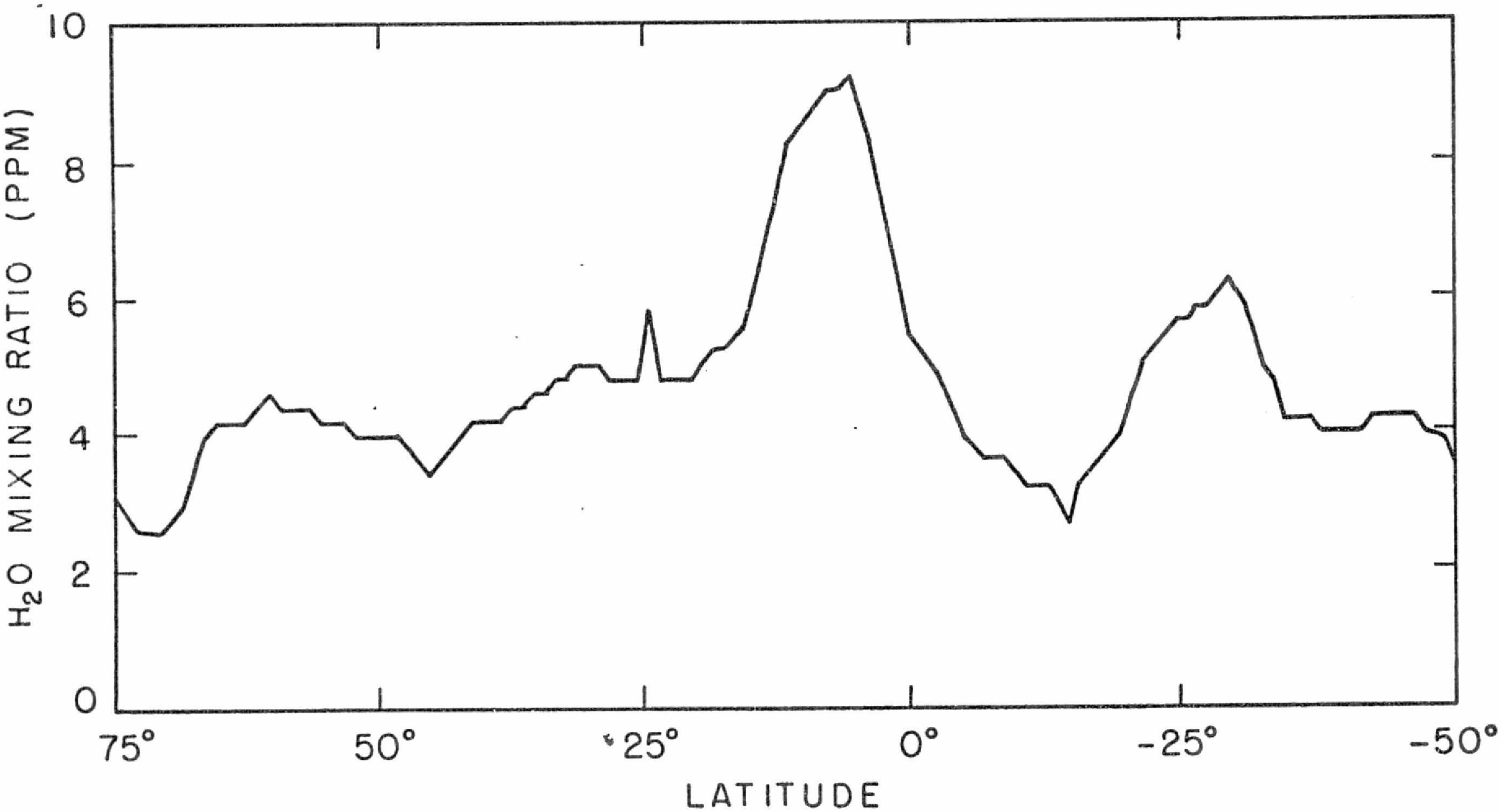

Figure 12

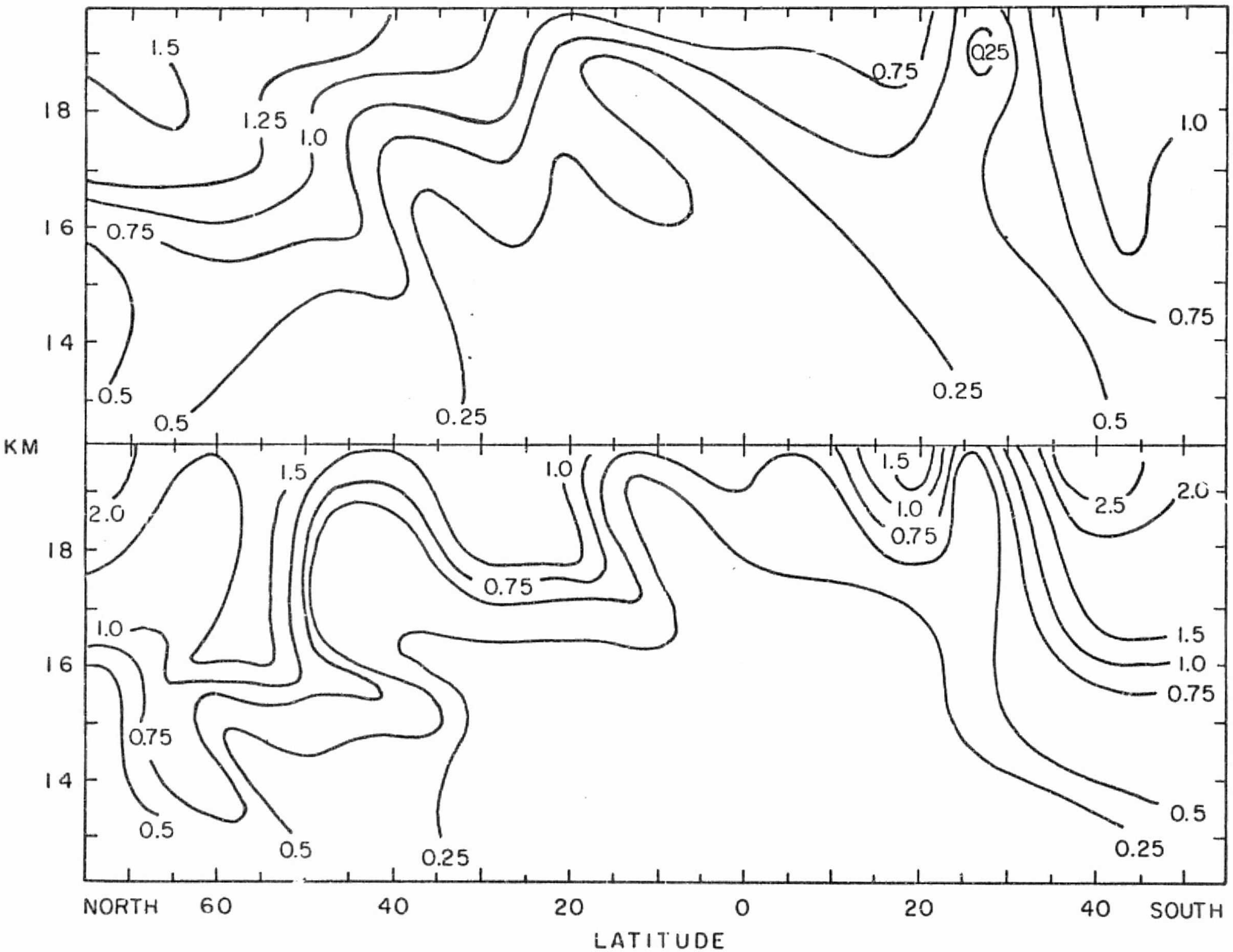
KM
18
16
14
1.5
1.25
1.0
0.75
0.5
0.25
2.0
2.5
NORTH
60
40
20
0
SOUTH
LATITUDE

Figure 13

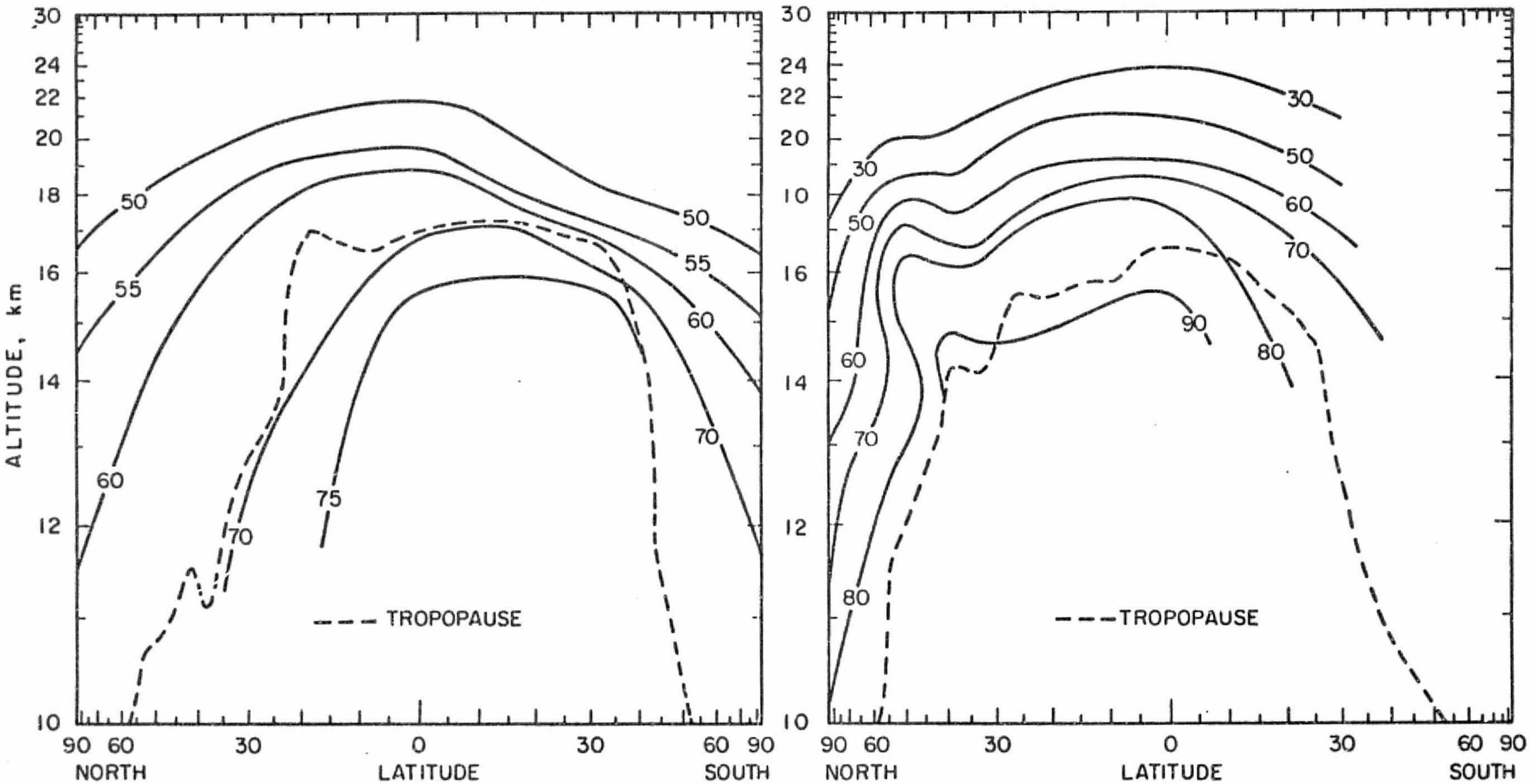

30
24
22
20
18
16
14
12
10
ALTITUDE, km
50
55
60
70
75
TROPOPAUSE
90 60
30
0
30
60 90
NORTH
LATITUDE
SOUTH
30
50
60
70
80
90
TROPOPAUSE

Figure 14

SIMULATION EXPERIMENTS ON THE CLIMATE OF THE STRATOSPHERE AND STRATOSPHERIC OZONE DISTRIBUTIONS UNDER NATURAL AND MAN-MADE CONDITIONS

F. N. Alyea, D. M. Cunnold, and R. G. Prinn

Department of Meteorology

Massachusetts Institute of Technology

Cambridge, Massachusetts 02139

Prepared for presentation at the Australian Conference on Climate and Climatic Change, December 7-11, 1975, Clayton, Victoria, Australia.

Although ozone (O_3) constitutes less than one-millionth of the mass of the atmosphere, it plays an important role in heating the stratosphere and in controling the amount of ultra-violet (UV) radiation that reaches the ground. The global distribution of O_3, however, evolves from a complex mixture of dynamical and chemical processes which lead to considerable spatial and temporal variations. Thus, in order to simulate the climatological changes in the stratosphere, a combined dynamical chemical three-dimensional model, global in scale, is desirable.

We are presently using such a model, 1) to simulate the large-scale climatological features and ozone distributions of the stratosphere, 2) to estimate the possible effects of anthropogenic pollution sources on the stratosphere and UV radiation levels at the surface, and 3) to study the dynamical and transport mechanisms relating to the stratosphere. To date some progress has been made relative to the first two of these points. Work has just begun on the third.

Model description

In order to accomplish these tasks, our strategy was to develop a fairly simple dynamical stratospheric circulation model (SCM) coupled with a relatively few chemical reactions considered most important to stratospheric O_3. The basic dynamical set of equations makes use of a form of quasi-geostrophic approximation. The chemistry is limited to the Chapman oxygen reactions

$$O_2 + h\nu \rightarrow 2O$$

$$O + O_2 + M \rightarrow O_3 + M$$

$$O_3 + h\nu \rightarrow O_2 + O$$

$$O + O_3 \rightarrow 2O_2$$

coupled with three odd nitrogen reactions

$$NO + O_3 \rightarrow NO_2 + O_2$$

$$NO_2 + O \rightarrow NO + O_2$$

$$NO_2 + h\nu \rightarrow NO + O$$

For details of the model see Cunnold, et al, (1975).

Although the model encorporates 26 vertical levels from the surface (including orographic effects) to approximately 72km height (well into the mesosphere), we are not concerned with reproducing the detailed observed motions in either the troposphere or the mesosphere. The troposphere has been included solely to provide a more or less realistic energy source to drive the stratosphere, while a number of model levels in the mesosphere have been retained in order to remove the upper boundary as far as possible from the stratospheric levels of interest. The 3-dimensional prediction variables are limited to vorticity, temperature, and ozone although, as in many other quasi-geostrophic models, horizontal mean temperatures are not predicted but are externally specified. Coupling between the photochemistry and the dynamics is achieved not only through the temperature-dependent photochemical reaction rates but also through the heating term in which the absorption of solar radiation by the predicted ozone is integrated explicitly using a simplified radiative transfer law. In the middle and upper layers of the model the radiative cooling is approximated using Newtonian rate coefficients computed by Dickinson (1973). Below about 20km (lower stratosphere and troposphere) heating is specified in a quite different manner. In earlier versions of the model this was accomplished through a simple linear parameterization of the Manabe and Strickler (1964) type in which the heating rate is proportional to the difference between an "equilibrium" temperature, T*, and the local model predicted temperature. Spatial and temporal distributions of T* were determined from data obtained from the M.I.T. General Circulation Project. Currently, however, we are replacing this linear heating mechanism with total heating data obtained from the results of a one year integration of the 13-layer general circulation model (GCM) of the Geophysical Fluid Dynamics Laboratory (GFDL) in Princeton, N.J. This procedure has the advantage of providing the model with a fairly detailed heating input, global in extent, and over the entire annual cycle. In contrast, the present heating parameterization is based on fairly smooth data which is limited to the Northern Hemisphere.

Horizontal representation of the model variables is accomplished by application of truncated series of spherical harmonics. To date all of the model computations have been limited to series representations which have been truncated after planetary wave number 6 (with equal resolution in the north-south direction). Higher resolutions are undoubtedly desirable but we appeal to the tendency for larger scales in the stratosphere. In addition, linear theory suggests that only the very long planetary scale waves of the troposphere penetrate far enough into the stratosphere to act as a major energy source for stratospheric motion.

Because of a lack of good tropospheric heating data in the Southern Hemisphere, it was convenient for the first few model integrations to assume that the two hemispheres are geographically similar. Thus, the orographic heights were defined by imagining that the Southern Hemisphere is a mirror image of the Northern Hemisphere (Fig. 1). Tropospheric heating values from the Northern Hemisphere are also used in the Southern Hemisphere, but with a six month time lag. In this way we have retained realistic interactions between the hemispheres while making use of the limited tropospheric heating data available.

Simulation of the unperturbed stratosphere

The initial model integrations were concerned with obtaining a fairly realistic climate simulation of the observed stratosphere. The model was integrated for a period of 3 years, starting from an initial state of rest, until the O_3 and dynamical quantities arrived at equilibrium solution conditions. Figure 2 shows a winter-summer seasonally averaged temperature cross-section obtained from year three (season 10) of the results of one of these model runs (Run 12). The upper part of this figure contains the corresponding observational analysis of Newell (1969). Throughout the stratosphere the model temperatures appear adequate, with some exceptions near the poles. Near the winter pole the model predicts temperatures that are approximately 20 degrees too low at upper and middle stratospheric levels. At the lowest stratospheric levels (~10-20km) both polar regions of the model exhibit temperatures somewhat higher than observations (by approximately 10-20 degrees). However, the probability of an error in the observational analysis exists at about 50km in the summer hemisphere (Newell, personal communication). Here the observational cross-section shows a closed 273°K contour which is about 20 degrees cooler than other independent observations and also as predicted by the model. In the lower mesosphere, the model fails to predict the observed reversal of the pole to pole temperature gradient. This probably results from the artificially imposed upper boundary condition in which the vertical pressure velocity is assumed to be zero.

Corresponding cross-sections for the seasonally averaged zonal wind field (winter-summer) are contained in Fig. 3. The data is as expected from the temperature profiles and the thermal wind relationship. The climatological winter-summer mean zonal winds obtained from the model exhibit the essential large-scale characteristics of stratospheric motion. A winter-hemisphere upper tropospheric (lower stratospheric) westerly jet, with maximum wind speeds of 40 m/s, is found at an altitude of 10km in the subtropics (although about 15° too far toward the equator). In the upper part of the stratosphere, a westerly wind belt (polar night jet) exists in winter, while easterlies prevail during the summer. The failure for the model upper stratospheric wind belt contours to close with the height above the $\sim$60km level is again attributed to the artificial upper boundary condition.

Another important climate parameter, and one that is certainly important to the transport of stratospheric ozone, is represented by the meridional mass circulation. Calculations of this quantity from atmospheric wind data have been made by Louis (1974). Figure 4 shows Louis' mass meridional circulation pattern for the winter-summer months, December through February. We see that the troposphere contains six individual circulation cells dominated by the direct (Hadley) tropical cell of the winter hemisphere. However, above the tropopause there is a rather abrupt change to a three cell (possibly four cell) pattern. Here again, the direct circulation pattern associated with the tropospheric winter hemisphere Hadley cell dominates, but has now extended its influence throughout the subtropics and into the midlatitudes of both hemispheres. The corresponding mass circulation pattern for the months December through February from the model calculations are contained in Figure 5. The results are essentially as computed by Louis, but the direct tropical cell in the summer hemisphere extends upwards through the entire stratosphere instead of being confined to the lower stratospheric levels noted in the observations. Nevertheless, the model exhibits a large stratospheric mass transport across the equator from the summer hemisphere to the winter hemisphere. This is in accord with the observational evidence and thus provides a satisfactory basic meridional flow field for the initial poleward transport of stratospheric O_3 away from the equatorial production regions.

Model ozone distributions

Coupled with the dynamical aspects treated above, the model also predicts three-dimensional O_3 distributions. In addition to transport of O_3 by the wind fields, the model O_3 quantities are also effected by temperature dependent chemical reactions. Feedback to the dynamics occurs through the heating terms which depends upon the absorption of solar radiation by the O_3.

An important contribution to the quantity of O_3 which exists in the stratosphere is realized through the presence of odd nitrogen compounds. NO reacts with ozone to destroy it by producing NO_2 and O_2, but the NO_2 is quickly converted to NO again. Thus, a catalytic reaction chain is realized in which the net result is O_3 depletion while the amount of NO remains unaltered. This odd nitrogen reaction chain has only recently been suggested as being important to stratospheric O_3 distributions and its absence from earlier model calculations undoubtedly accounts for their overprediction (by about a factor of 2) of O_3.

Since our model does not explicitly predict odd nitrogen, we are forced to provide spatial and temporal odd nitrogen distributions from independent sources. For the model results to be discussed here, we have adopted NO_2 values as predicted by a two-dimensional model calculation of Hesstvedt (1974), from which NO is obtained diagnostically. This NO_2 distribution, at its midsummer and midwinter extremes, is shown in Fig. 6. The values lie within the range of uncertainty (about a factor of 2) of the limited number of measurements, and we therefore consider them adequate as a first estimate. We note from the figure that the NO_2 mixing ratios appear to be relatively independent of latitude, but vary considerably with height, attaining maximum values at about 35km.

Figure 7 includes mean zonal O_3 cross sections for the winter-summer (December through February) season from observations (Wu, 1973) and from the model calculations. The model correctly predicts the downward and poleward transport of ozone, with maximums at polar latitudes. However, in the model, these maximum densities are located about two kilometers too high. This undoubtedly results from an inadequate downward transport of O_3 into the troposphere by eddy motions which are restrained by the model's limited resolution (truncated after planetary wave 6). As another basis for comparison of observations with our model O_3 results, we refer to Fig. 8 in which total columnar O_3 values, as a function of latitude and season for the Northern Hemisphere, are shown. An observational compilation by Dütsch (1971) is presented in the upper part while a similar picture, averaged over year 3 of the model results, is contained in the lower part of this figure. The model has correctly simulated the observed polar spring maximum as well as the relative minimum at the pole in the fall. The polar spring maximum, however, is some 10% less than is observed, reaching just over 400 Dobson units compared to more than 440 in the observations.

Ozone reduction by SST's

Since the amount of O_3 in the stratosphere is somewhat controled by the presence of odd nitrogen compounds, it stands to reason that aircraft, whose engines produce odd nitrogen compounds, flying in the stratosphere may inject quantities of odd nitrogen sufficient to be of importance to the O_3 balance. This is of particular concern because of the relatively long time periods required for the net removal of odd nitrogen at these altitudes. Such long residence times are primarily due to the inherent vertical thermal stability of the stratosphere. The principle removal mechanism for odd nitrogen in the stratosphere appears to involve its conversion to nitric acid (HNO_3), with subsequent transport into the troposphere and rainout. Thus, it is important that we obtain an estimate of the long-range effect on the O_3 layer that might be generated by a large fleet of supersonic transports (SST's), before such a fleet becomes a reality.

To do this, we have introduced an additional amount of NO_2 into the model to represent a hypothetical SST fleet (Alyea, et al, 1975). This perturbation in NO_2 was computed using a two-dimensional model for chemical stratospheric constituents developed by us at M.I.T. (Prinn, et al, 1975). For this first perturbed NO_2 calculation, we assumed an odd nitrogen emission rate of 1.8×10^6 metric tons per year, to be released in a corridor centered at 45° N and an altitude of 20 km. The corridor extends 15° in latitude and 1 km in height. This injection rate was chosen to most nearly represent the effect of a large fleet ($\sim$500 aircraft) of the now cancelled American SST (Boeing 2707) which might have existed near the year 2000. The results of the two-dimensional calculation of the NO_2 perturbation, after equilibrium solutions had been obtained (some 25 years of integration time), are shown in Fig. 9 (Northern Hemisphere winter). We see that while much of the introduced odd nitrogen is found in the Northern Hemisphere, interhemispheric transport processes have distributed a significant quantity to the Southern Hemisphere, particularly in the 30-40km altitude range.

The effect of this increased amount of odd nitrogen introduced into the stratosphere can be seen in the O_3 distribution simulated by the three-dimensional model. Figure 10 shows the seasonally averaged distributions of total columnar O_3 as a function of latitude, calculated for both the SST-perturbed stratosphere and the unperturbed stratosphere. On a global scale the perturbed stratospheric O_3 depletion amounts to about 12%. However, the model also shows that about 16% of the Northern Hemisphere O_3 will be destroyed. Despite the absence of any direct odd nitrogen injection in the Southern Hemisphere, the calculations indicate that approximately 8% of the total O_3 will be destroyed there. The mid-latitude injection of odd nitrogen in the Northern Hemisphere apparently produces a filtering effect on the northward transport of O_3 through this region so that there is a larger (by about a factor of 2) reduction of O_3 at high northern latitudes than at low latitudes.

To estimate UV radiation reaching the ground, we submitted the total O_3 distributions for the January and July months to Dr. S. V. Venkateswaran, who used this data in a multiple scattering program (N. Sundararaman, <u>et al.</u>,

1975) to compute daily mean surface UV flux values. The values for both the unperturbed and perturbed stratosphere at four wavelengths under clear sky conditions were then used to prepare curves of approximate erythermal dosage (sunburn producing effect on Caucasian skin). If $F(\lambda)$ represents the solar UV flux per unit wavelength arriving at the ground, then the erythermal dose D at a given latitude and time of year can be represented by

$$D = \int_{\lambda} E(\lambda)\ F(\lambda)\ d(\lambda)$$

where $E(\lambda)$ denotes an erythermal efficiency function (e.g., Cutchis, 1974, Fig. 8). The results of the numerical integration of this equation for the July and January months for which UV fluxes were obtained are shown in Fig. 11. The greatest differences between the calculations for the perturbed and unperturbed states occur during July in the Northern Hemisphere. The erythermal dose at 30°N for the perturbed state is about 30% greater than that for the unperturbed state. At 60°N this difference increases to about 58%. Thus, during July the calculations indicate that Northern Hemisphere mid-latitude erythermal doses under the perturbed conditions are roughly equivalent to unperturbed levels some 15° of latitude to the south. At the same time, Southern Hemisphere July mid-latitude erythermal radiation levels are relatively uneffected. During January, however, mid-latitude erythermal doses in the Southern Hemisphere are comparable to an equatorward latitudinal shift of about 7°. In Melbourne, which is somewhat on the equatorward side of the central mid-latitudinal belt, the summer sunburn potential under these perturbed conditions would be roughly equivalent to that of present day New Caledonia or along central sections of the Great Barrier Reef.

Two additional model calculations have been made concerning the possible effects on the O_3 layer due to operation of an SST fleet of aircraft. On of these (Run 19) assumes that the SST corridor is centered at an altitude of 17km (rather than 20km as in Run 18) at 45°N, while the other calculation assumes a tropical flight corridor at 20km altitude and 10°N. Summer and winter seasonally averaged distributions of total columnar O_3 as functions of latitude for these two experiments (Runs 19 and 20), as well as for the unperturbed (Run 17) and the 20km, 45°N SST corridor (Run 18) cases are compared in Fig. 12. The calculations show that for the conditions of Run 19 (corridor at 17km, 45°N), approximately 6% of the total unperturbed O_3 will be destroyed during an annual cycle. Most of this depletion occurs in the Northern Hemisphere where 8% of the total O_3 contained there will be lost. In contrast, only about 3% depletion will occur in the Southern Hemisphere. This is particularly evident during the Northern Hemisphere winter and summer seasons shown in Fig. 12 during which 11% (N. H. winter) and 8% (N. H. summer) O_3 depletions are indicated. At the same time, negligible O_3 losses are noted in the Southern Hemisphere. Thus, we see, in comparison with the results of Run 18, that lowering the altitude at which a fleet of SST's would operate reduces its impact on O_3 depletion in the Southern Hemisphere,but still must be considered as a factor in the Northern Hemisphere.

The situation is somewhat different, however, when SST's fly in the tropics,as simulated in Run 20 (corridor at 20 km, 10°N). For this case approximately 12% of the total global O_3 will be destroyed throughout the year (the same amount as obtained from Run 18), but this loss is fairly evenly distributed between the two hemispheres. This feature can be seen in Fig. 12, especially for the Northern Hemisphere summer during which the difference between the unperturbed curve (Run 17) and the Run 20 perturbed curve is fairly uniform from pole to pole.

The odd nitrogen injection rate assumed in our model calculations (1.8×10^6 metric tons per year) was chosen to most nearly represent the effect of a rather large fleet (about 500 aircraft) of the proposed Boeing 2707 SST, which might have existed near the year 2000. However, if, in fact, only SST's of the current Anglo-French Concorde and Russian Tupolev 144 prototypes, which are smaller and fly at lower, less harmful altitudes ($\sim$17 km), are built, we estimate that it would require a world wide fleet of a few thousand aircraft to attain an effective injection rate as large as the one used in our model simulation. Clearly, the nature and proliferation of the global SST fleet of the future must be carefully analysed if we intend to maintain the environment as we know it today.

References

Alyea, F.N., D. M. Cunnold, and R.G. Prinn, 1975: Stratospheric ozone destruction by aircraft-induced nitrogen oxides. Science, 188, 117-121.

Cunnold, D., F. Alyea, N. Phillips, and R. Prinn, 1975: A three-dimensional dynamical-chemical model of atmospheric ozone. J. Atmos. Sci., 32, 170-194.

Cutchis, P., 1974: Stratospheric ozone depletion and solar ultraviolet radiation on earth. Science, 184, 13-19, figure 8.

Dickinson, R. 1973: A method of parameterization for infra-red cooling between altitudes of 30 and 70 km. J. Geophys. Res., 78, 4451-4457.

Dutsch, H., 1971: Photochemistry of atmospheric ozone. Advances in Geophysics, Vol. 15, Academic Press, 219-322.

Hessvedt, E., 1974: A simplified time-dependent two-dimensional photochemical model of the stratosphere. Proceedings of the International Conference on Structure, Composition and General Circulation of the Upper and Lower Atmospheres and Possible Anthropogenic Perturbations, Melbourne, Australia, January 14-25, 1974, Vol. II, 1097-1106.

Louis, J.-F., 1974: A two-dimensional transport model of the atmosphere. Ph.D. thesis, Department of Astro-Geophysics, Univ. of Colorado, Boulder, Colorado, pp. 150.

Manabe, S. and R. Strickler, 1964: Thermal equilibrium of the atmosphere with a convective adjustment. J. Atmos. Sci., 21, 361-385.

Newell, R., 1969: Radioactive contamination of the upper atmosphere. Progress in Nuclear Energy - Series XII, Health Physics, Vol. 2, A.M. Francis Duhamel, Ed, Pergannon, 535-550.

Prinn, R.G., F.N. Alyea, and D.M. Cunnold, 1975: Stratospheric distributions of odd nitrogen and odd hydrogen in a two-dimensional model, J. Geophys. Res., in press.

Sundararaman, N., D. St. John, and S. Venkateswaran, in preparation.

Figure titles

Fig. 1. Model surface topography in dekameters drawn from the truncated spectral representation.

Fig. 2. The atmospheric temperature distribution obtained for season 10, Run 12 compared against the observed atmospheric temperature distribution for summer and winter according to Newell (1969).

Fig. 3. Vertical cross section of the zonal wind (m/s) for season 10, Run 12 compared with the summer-winter observations analyzed by Newell (1969).

Fig. 4. Mean meridional circulation (mass flow in units of 10^{12} g/s) redrawn from an analysis by Louis (1974) for the months December-February.

Fig. 5. Mean meridional circulation patterns from the model results (Run 17, season 12) for the months December-February.

Fig. 6. The unperturbed winter-summer NO_2 distribution (in parts per billion by volume) according to Hesstvedt (1974).

Fig. 7. Ozone number density (10^{11}/cm) cross sections for the winter-summer season predicted by the model for season 12, Run 17 compared with observations analyzed by Wu (1973).

Fig. 8. Columnar O_3 distribution (in Dobson units) in the Northern Hemisphere as a function of season and latitude: (a) as determined by Dutsch (1971) from observations and (b) as predicted during year 3 (Run 17) in our unperturbed model.

Fig. 9. The winter-summer SST induced perturbation in NO_2 (in parts per billion by volume) from the two-dimensional model of Prinn, et al (1975).

Fig. 10. Seasonally averaged distributions of columnar O_3 (in Dobson units) as a function of latitude predicted for the unperturbed (dashed lines - Run 17) and perturbed (solid lines - Run 18) stratospheres.

Fig. 11. Approximate daily mean erythermal doses predicted from the model O_3 results shown in Fig. 10 but limited to the months of January and July.

Fig. 12. Same as Fig. 10 but adding the results of the SST hypothetically perturbed conditions of Runs 19 and 20 (see text for details).

MODEL SURFACE TOPOGRAPHY (dm)

DRAWN FROM SPECTRAL REPRESENTATION

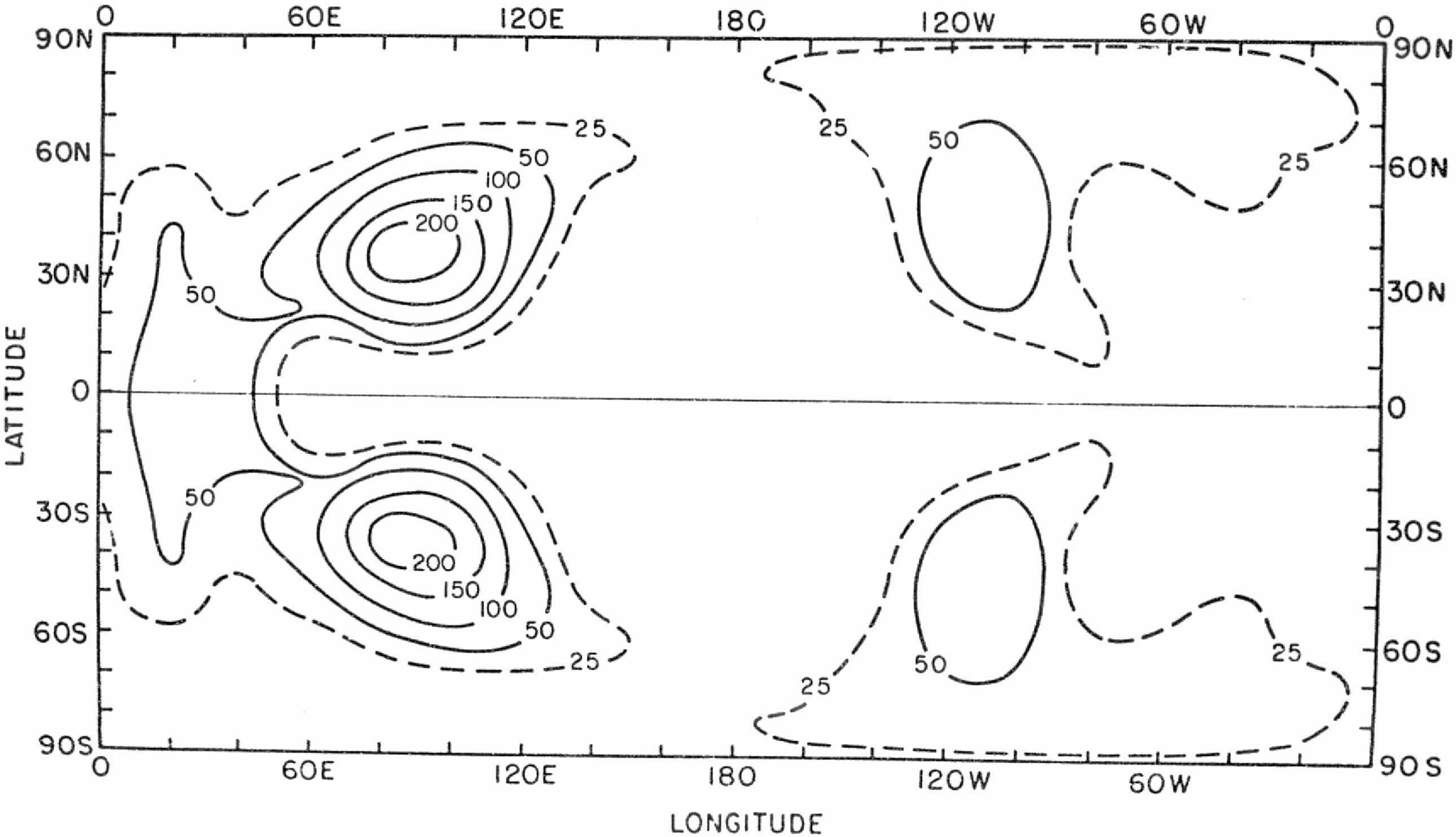

Fig. 1.

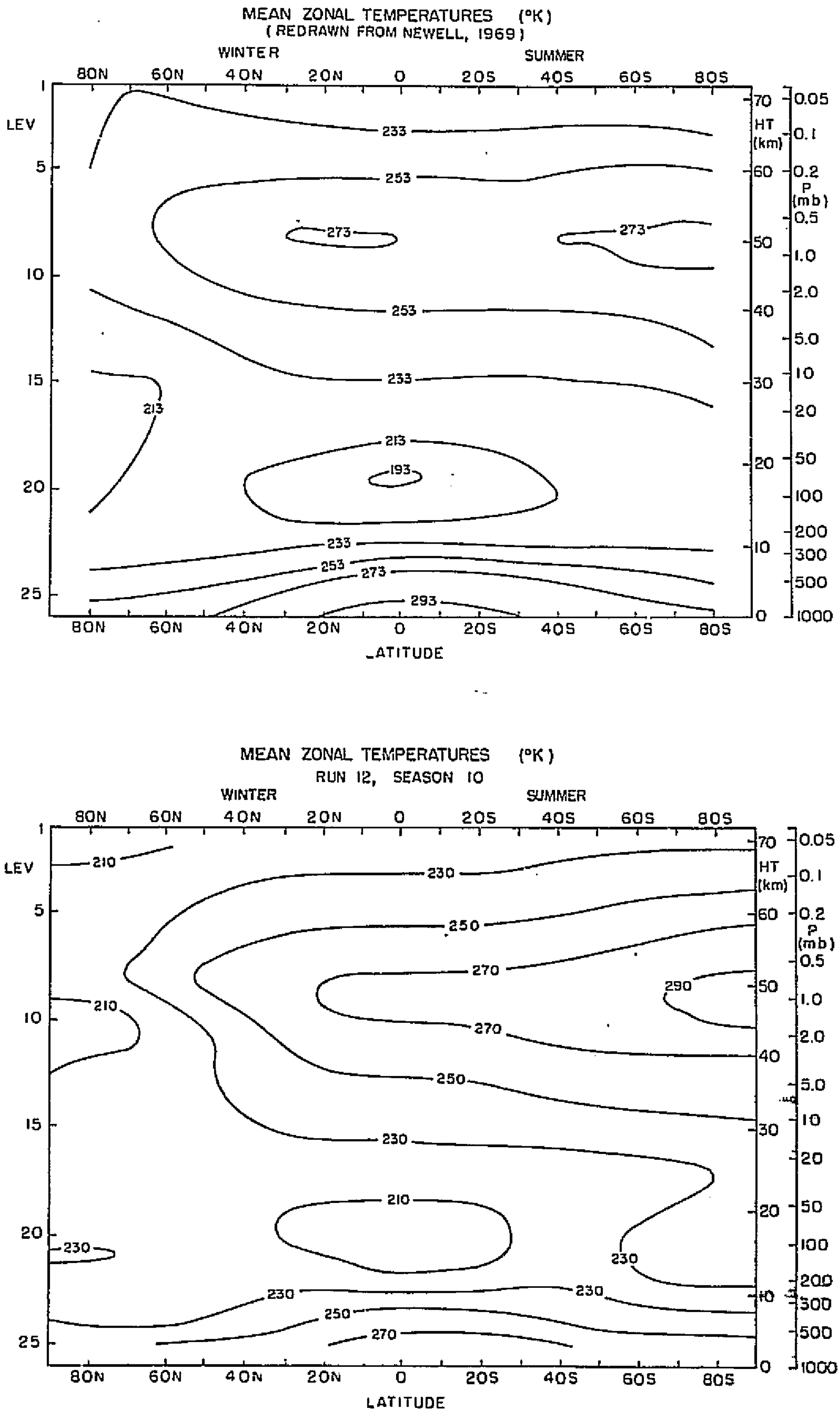
MEAN ZONAL TEMPERATURES (°K)
(REDRAWN FROM NEWELL, 1969)
WINTER
SUMMER
80N 60N 40N 20N 0 20S 40S 60S 80S
LEV
HT (km)
P (mb)
233
253
273
253
233
213
213
193
233
253
273
293
LATITUDE
MEAN ZONAL TEMPERATURES (°K)
RUN 12, SEASON 10
WINTER
SUMMER
210
230
250
270
290
270
250
230
210
210
230
230
230
230
250
270
LATITUDE

Fig. 2.

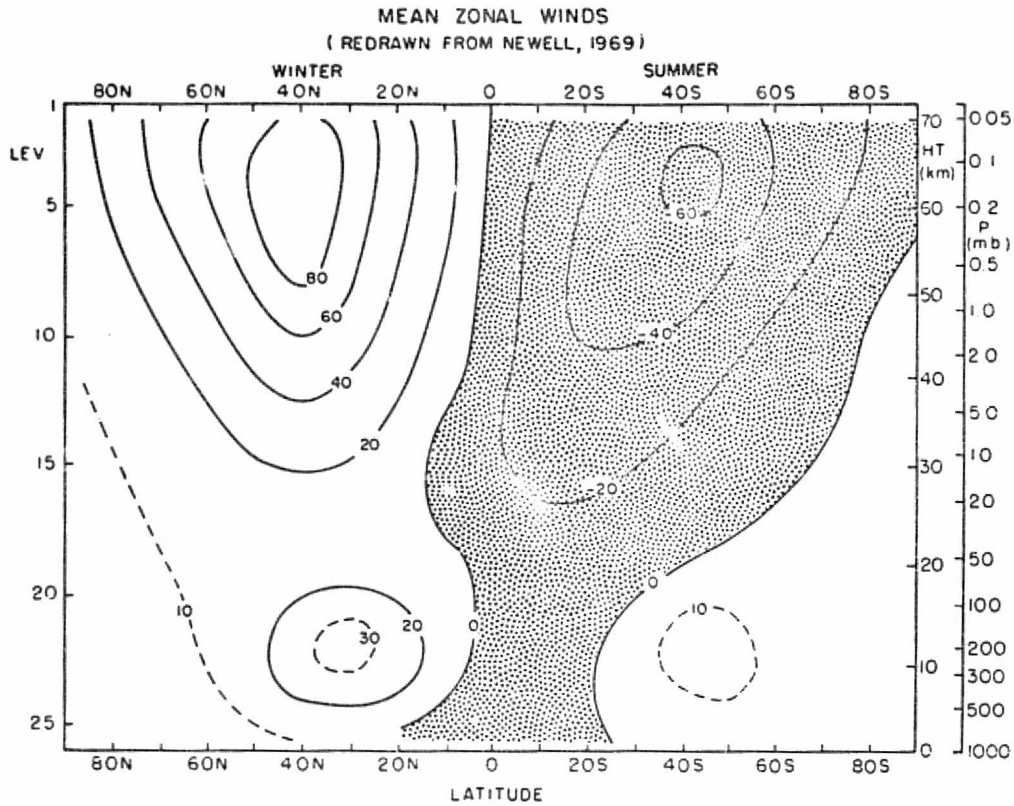
MEAN ZONAL WINDS
(REDRAWN FROM NEWELL, 1969)
WINTER
SUMMER
80N 60N 40N 20N 0 20S 40S 60S 80S
LEV
HT (km)
P (mb)
80
60
40
20
30
20
10
0
-60
-40
-20
-10
LATITUDE

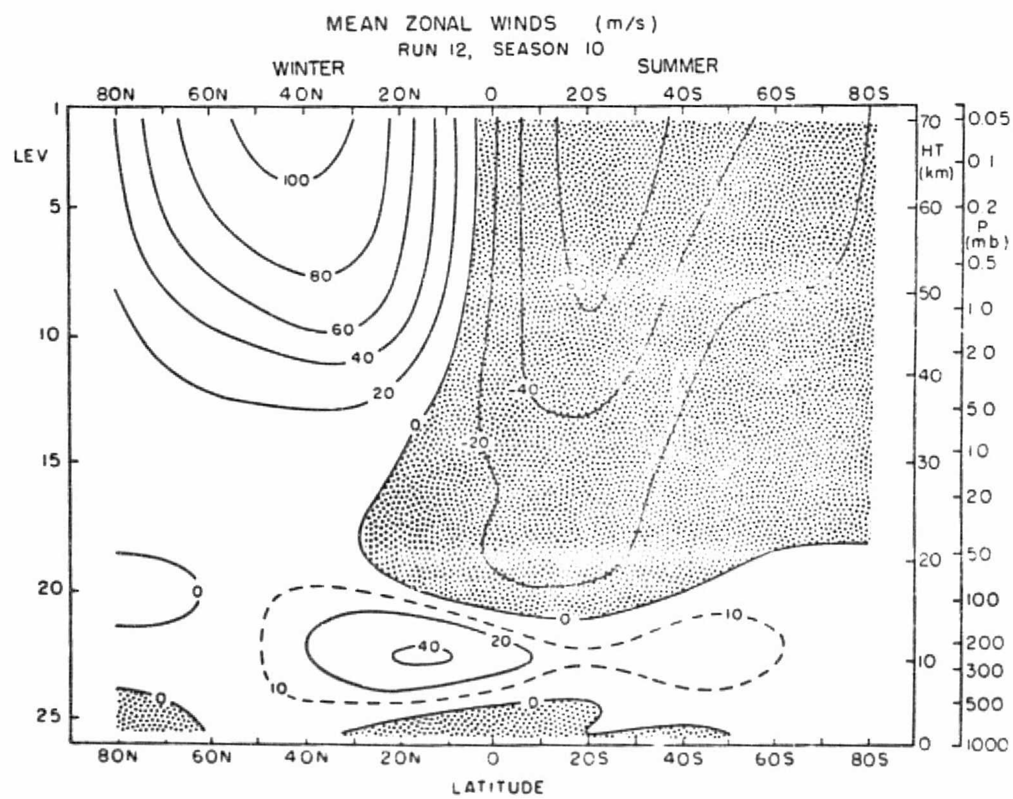
MEAN ZONAL WINDS (m/s)
RUN 12, SEASON 10
WINTER
SUMMER
80N 60N 40N 20N 0 20S 40S 60S 80S
LEV
HT (km)
P (mb)
100
80
60
40
20
0
-20
-40
40
10
LATITUDE

Fig. 3.

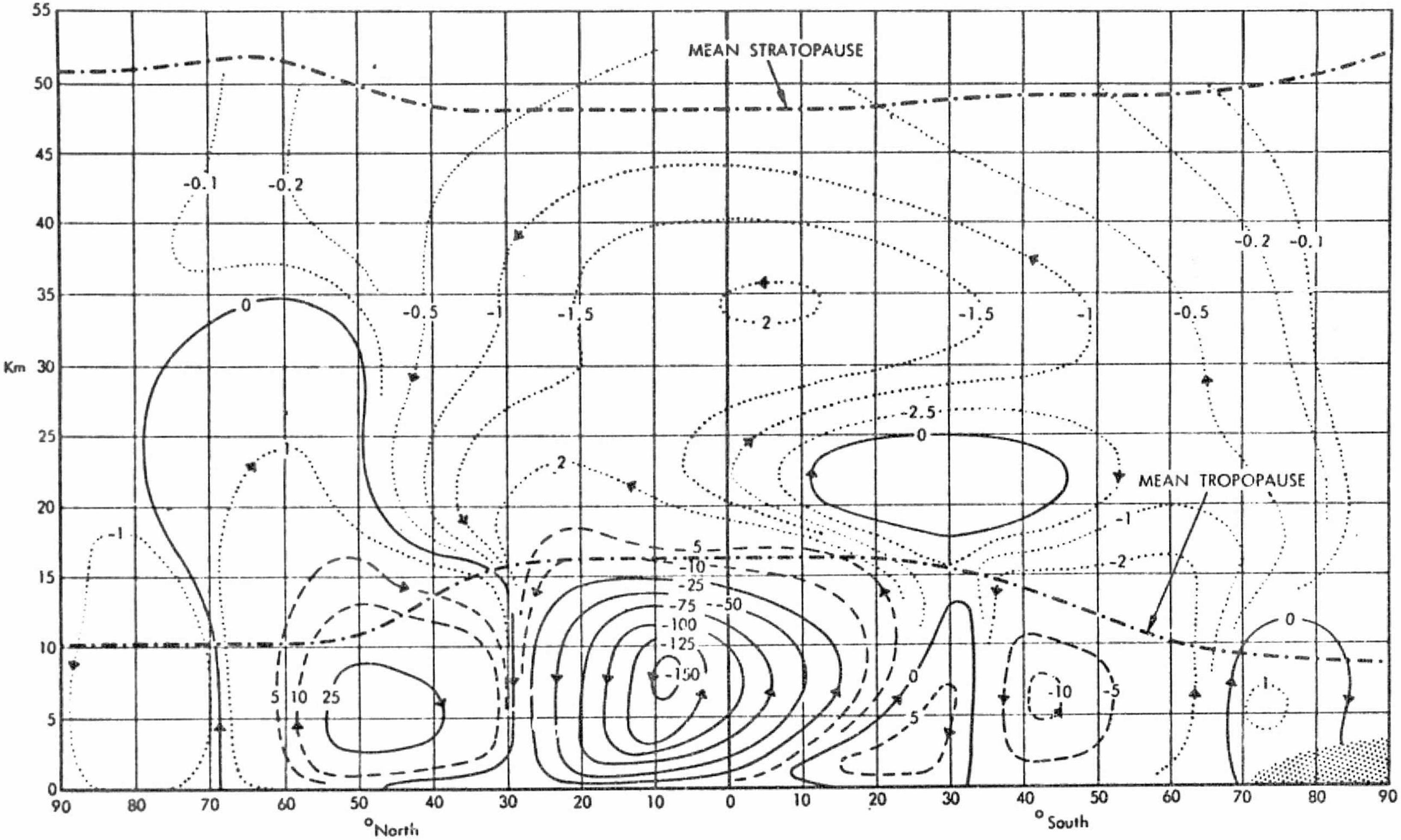

Fig. 4.

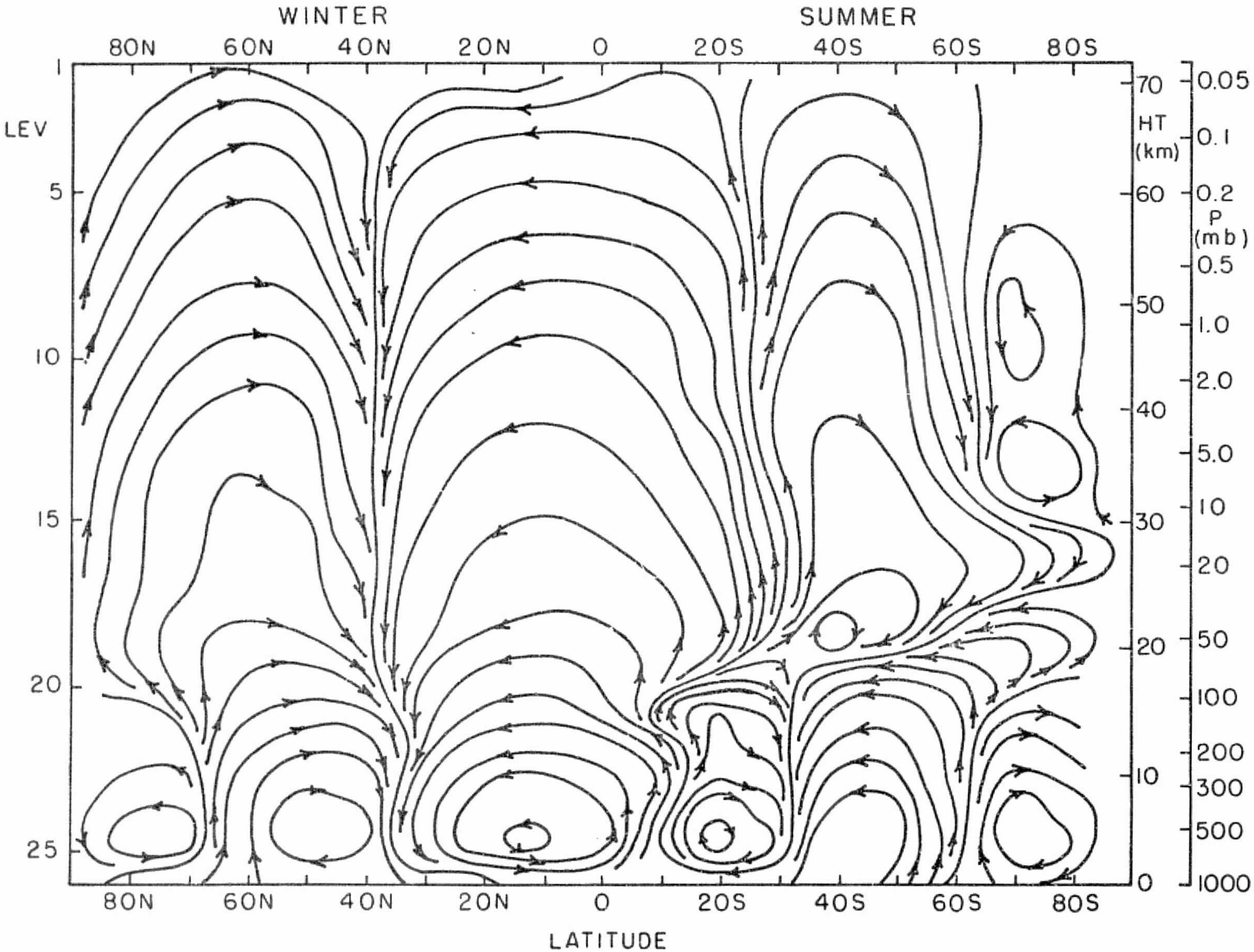
WINTER
SUMMER
80N
60N
40N
20N
0
20S
40S
60S
80S
LEV
1
5
10
15
20
25
HT (km)
70
60
50
40
30
20
10
0
P (mb)
0.05
0.1
0.2
0.5
1.0
2.0
5.0
10
20
50
100
200
300
500
1000
LATITUDE

Fig. 5.

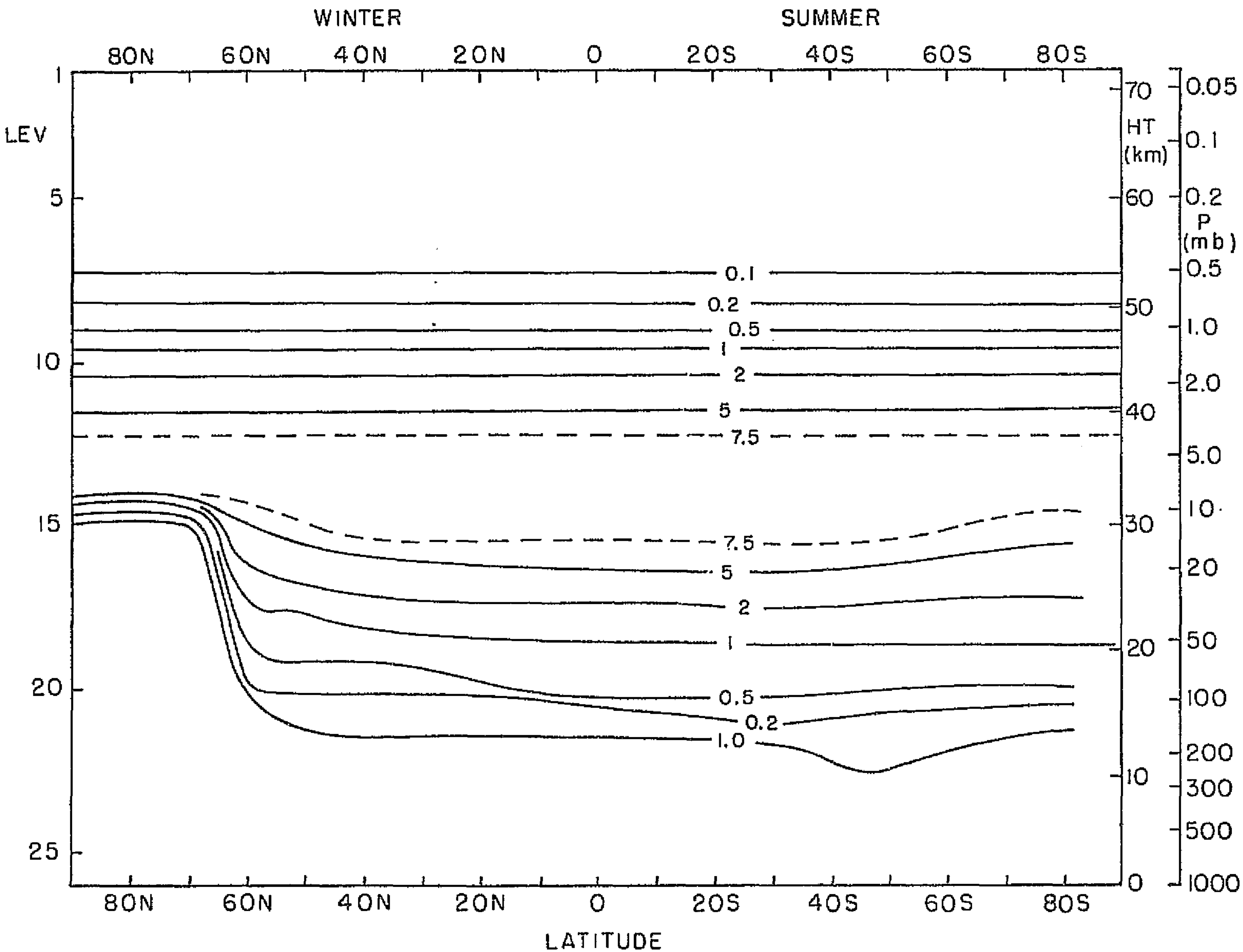
WINTER
SUMMER
80N
60N
40N
20N
0
20S
40S
60S
80S
LEV
1
5
10
15
20
25
HT (km)
70
60
50
40
30
20
10
0
P (mb)
0.05
0.1
0.2
0.5
1.0
2.0
5.0
10
20
50
100
200
300
500
1000
0.1
0.2
0.5
1
2
5
7.5
7.5
5
2
1
0.5
0.2
1.0
LATITUDE

Fig. 6.

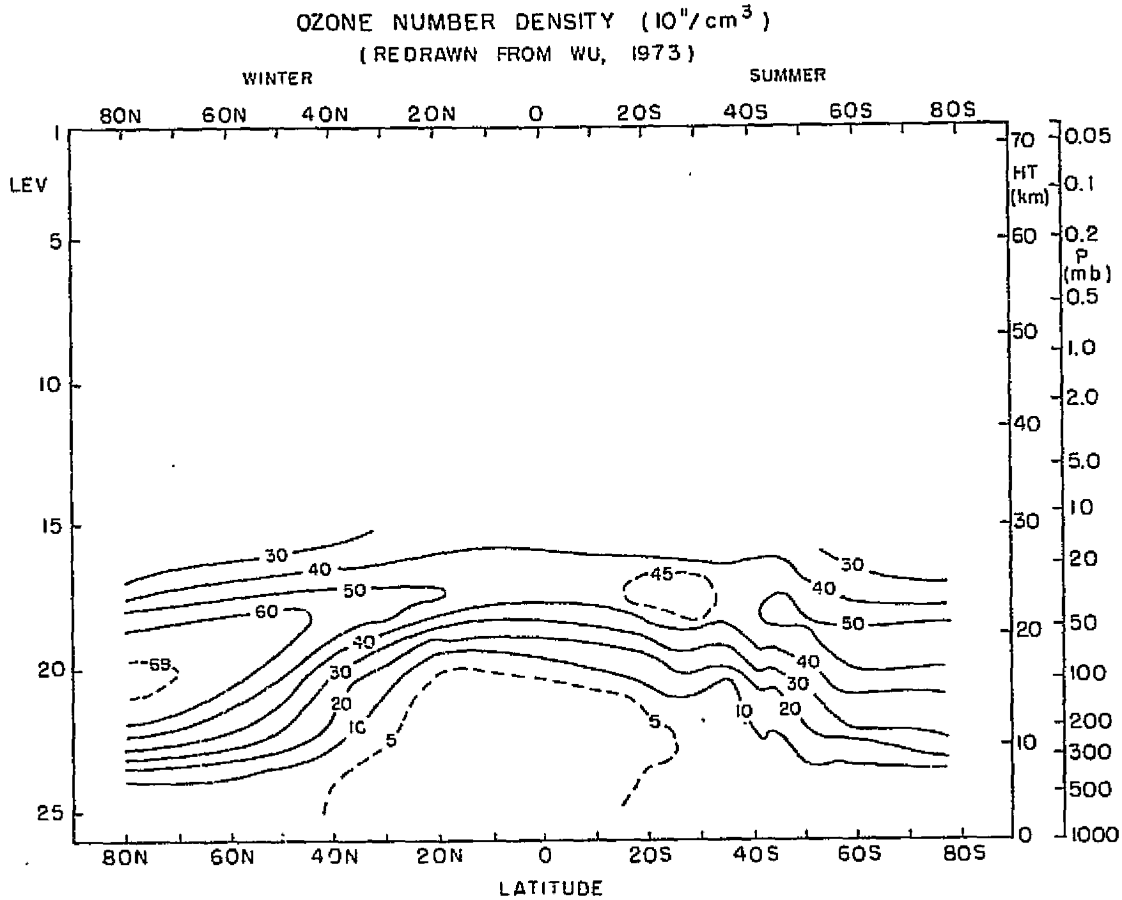

OZONE NUMBER DENSITY ($10^{11}/cm^3$)
(REDRAWN FROM WU, 1973)
WINTER
SUMMER
80N 60N 40N 20N 0 20S 40S 60S 80S
LEV
HT (km)
P (mb)
LATITUDE

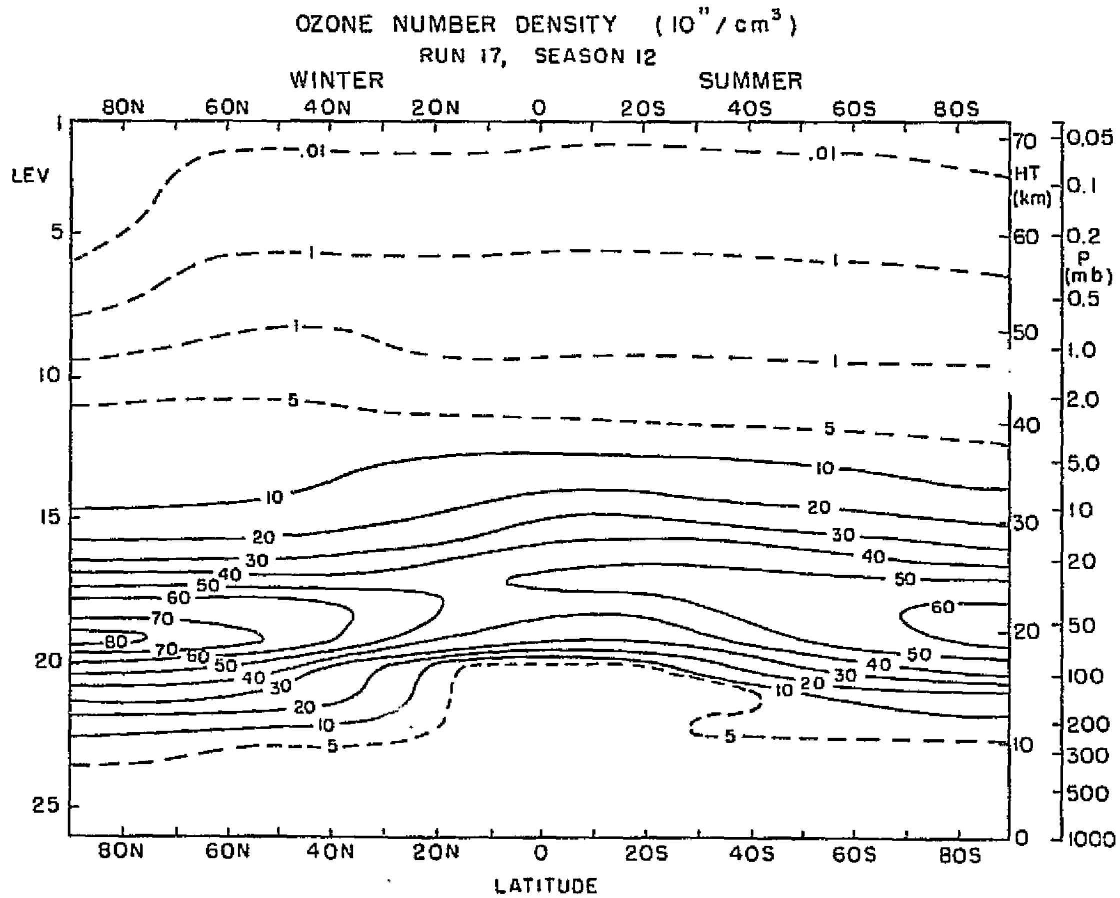

OZONE NUMBER DENSITY ($10^{11}/cm^3$)
RUN 17, SEASON 12
WINTER
SUMMER
80N 60N 40N 20N 0 20S 40S 60S 80S
LEV
HT (km)
P (mb)
LATITUDE

Fig. 7.

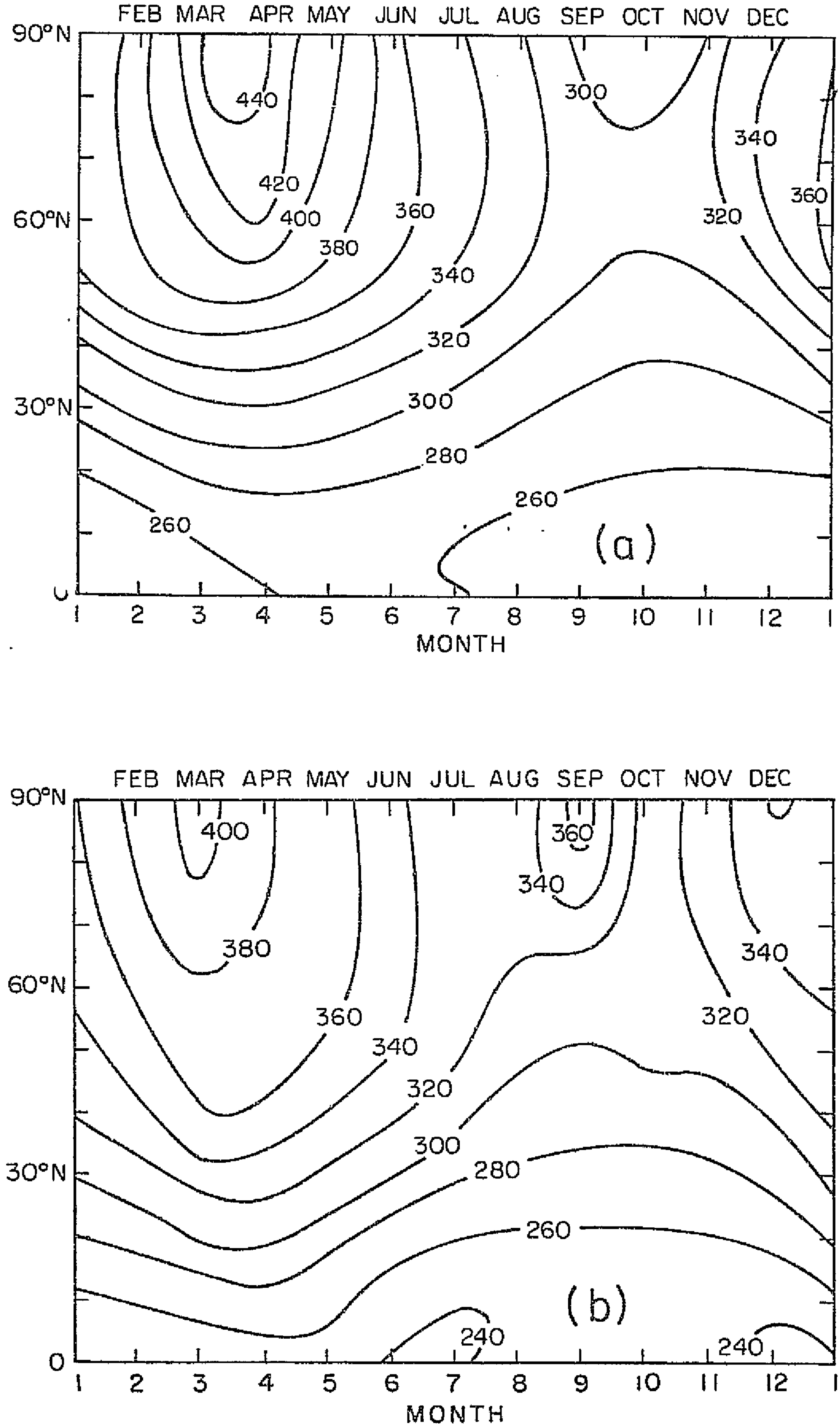
FEB MAR APR MAY JUN JUL AUG SEP OCT NOV DEC
90°N
60°N
30°N
0
440
420
400
380
360
340
320
300
280
260
(a)
1 2 3 4 5 6 7 8 9 10 11 12 1
MONTH
FEB MAR APR MAY JUN JUL AUG SEP OCT NOV DEC
90°N
60°N
30°N
0
400
380
360
340
320
300
280
260
240
(b)
1 2 3 4 5 6 7 8 9 10 11 12 1
MONTH

Fig. 8.

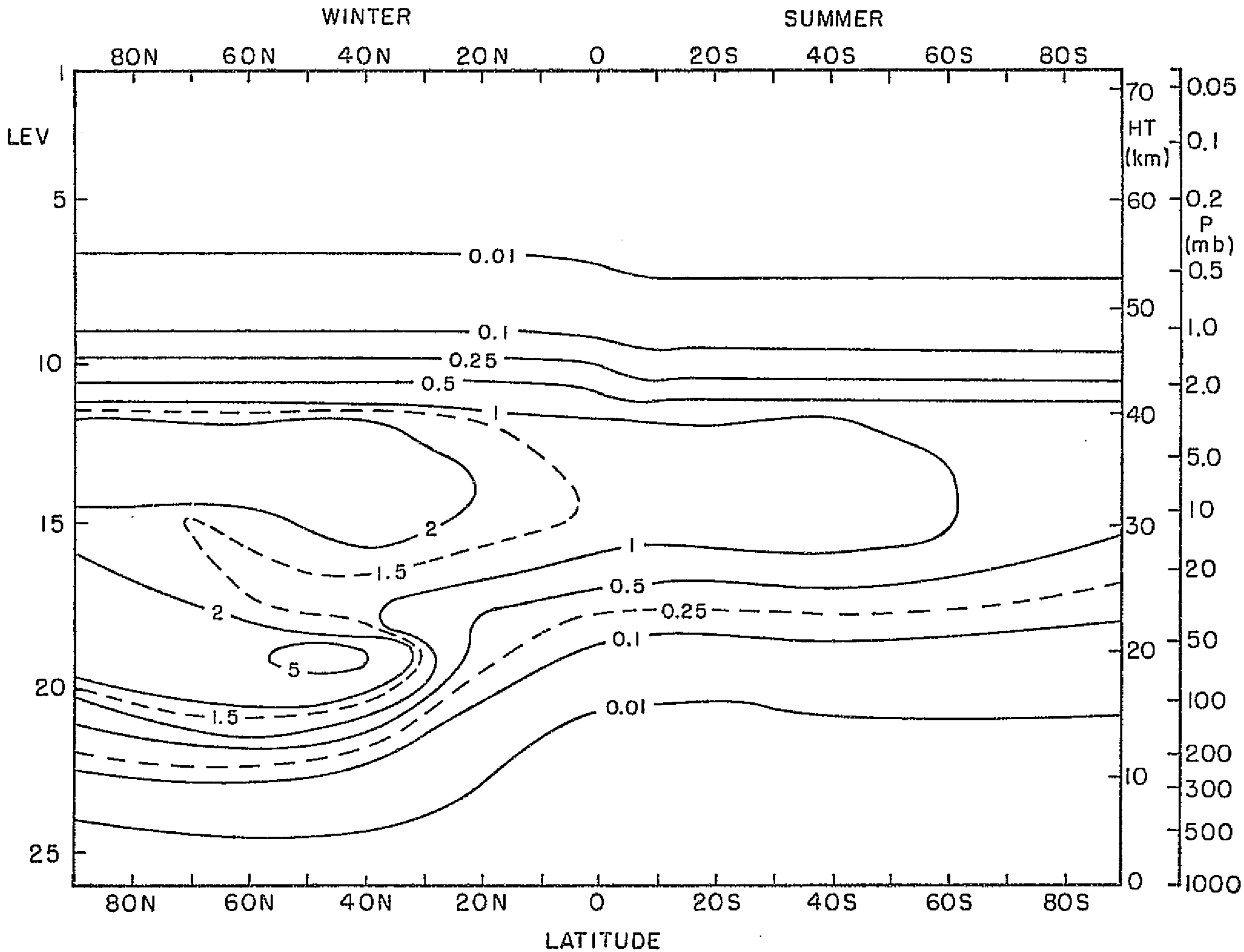

WINTER
SUMMER
80N 60N 40N 20N 0 20S 40S 60S 80S
LEV
1
5
10
15
20
25
HT (km)
70 60 50 40 30 20 10 0
P (mb)
0.05 0.1 0.2 0.5 1.0 2.0 5.0 10 20 50 100 200 300 500 1000
0.01
0.1
0.25
0.5
1
2
1.5
5
LATITUDE

Fig. 9.

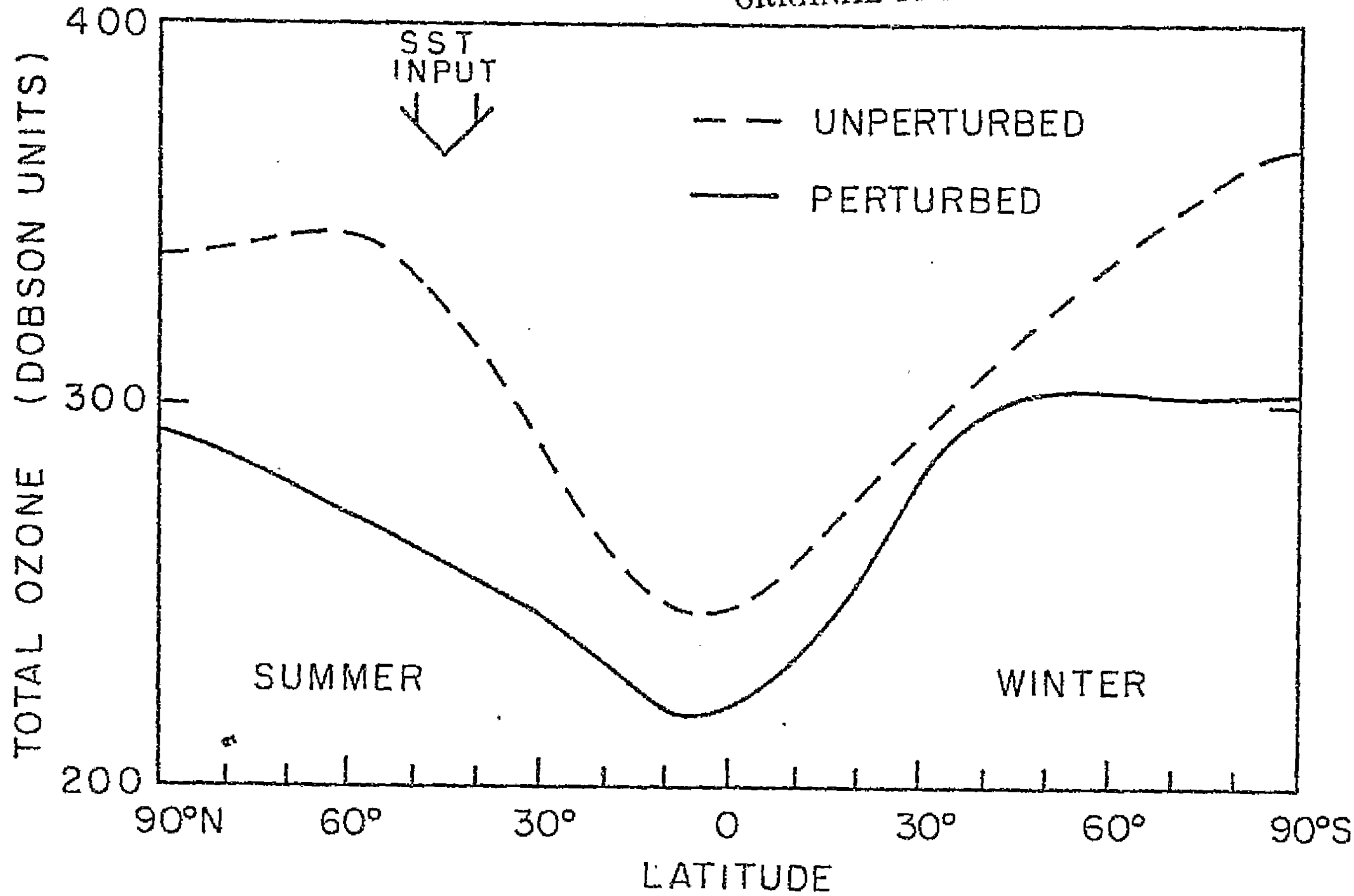
400
300
200
SST
INPUT
UNPERTURBED
PERTURBED
SUMMER
WINTER
TOTAL OZONE (DOBSON UNITS)
90°N
60°
30°
0
30°
60°
90°S
LATITUDE

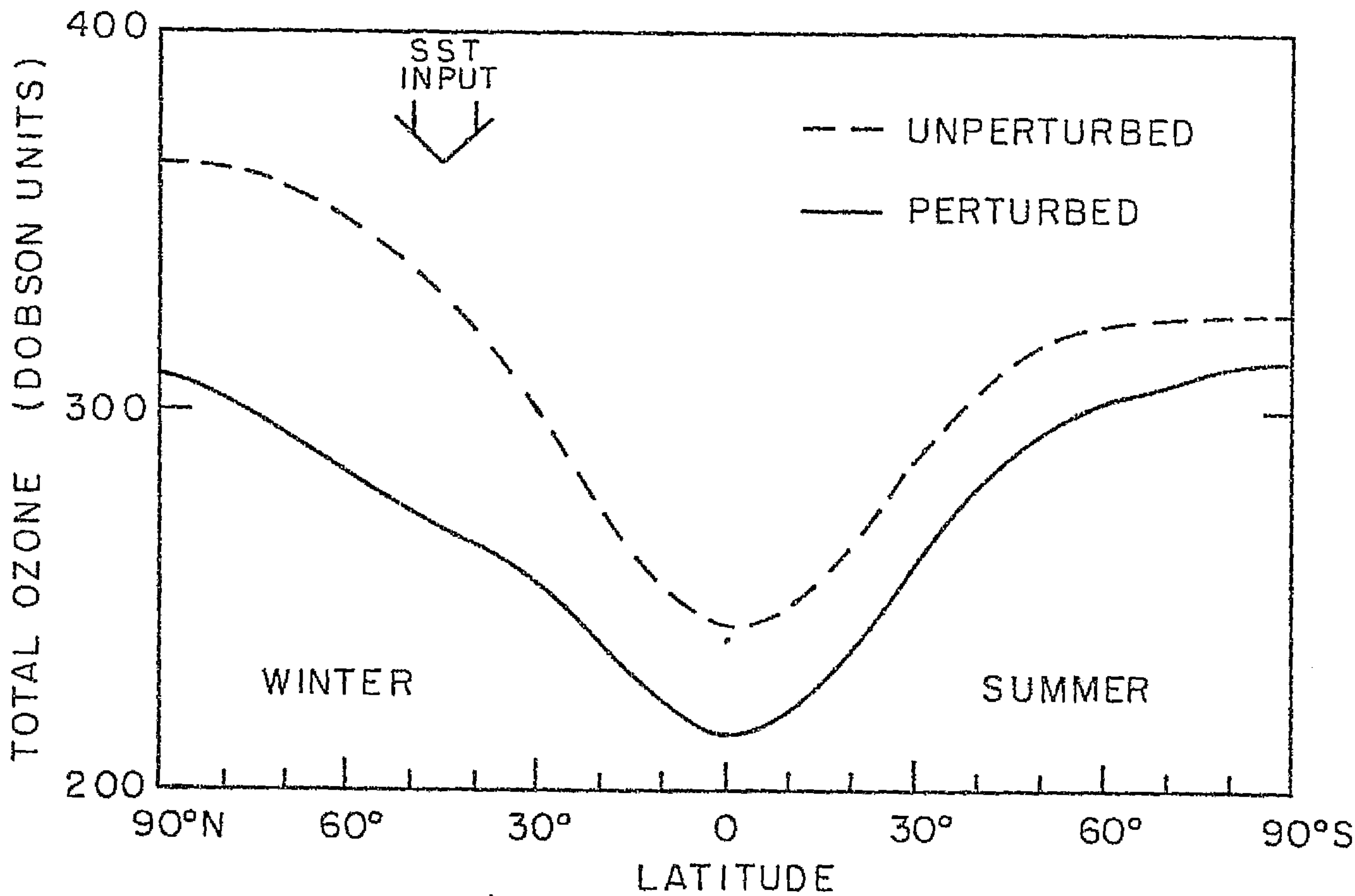
400
300
200
SST
INPUT
UNPERTURBED
PERTURBED
WINTER
SUMMER
TOTAL OZONE (DOBSON UNITS)
90°N
60°
30°
0
30°
60°
90°S
LATITUDE

Fig. 10.

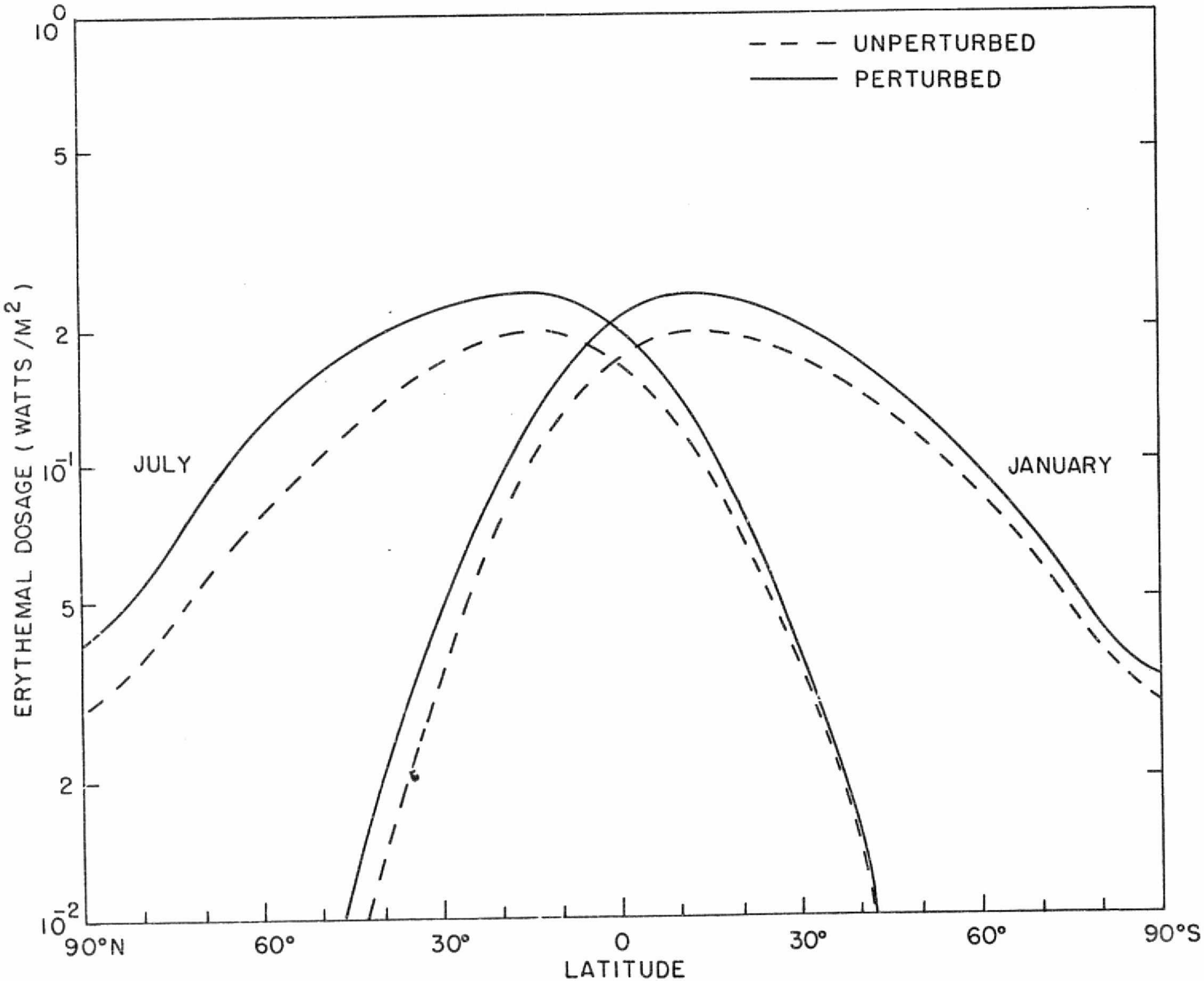
UNPERTURBED
PERTURBED
JULY
JANUARY
ERYTHEMAL DOSAGE (WATTS /M^2)
10^0
5
2
10^{-1}
5
2
10^{-2}
90°N
60°
30°
0
30°
60°
90°S
LATITUDE

Fig. 11.

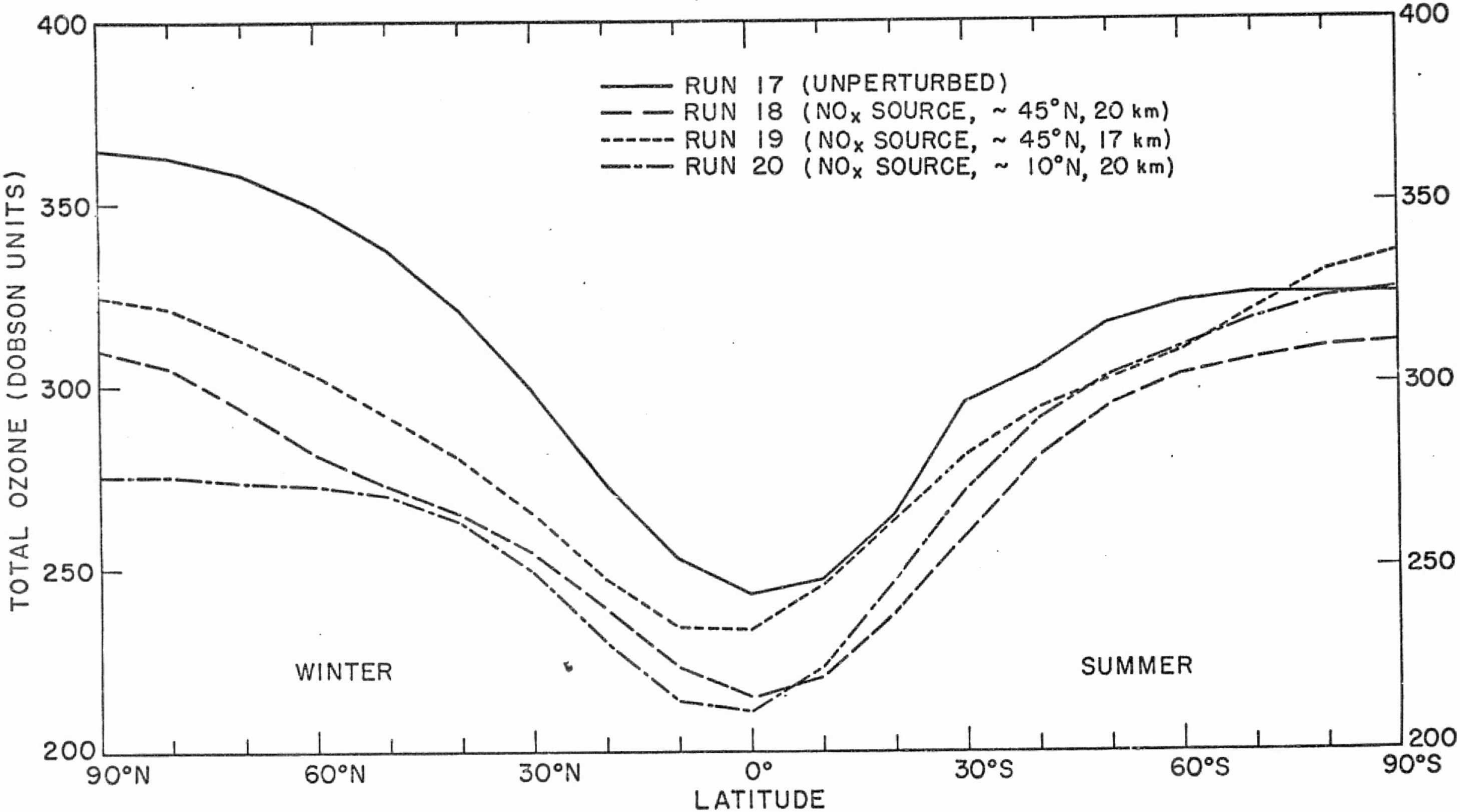
RUN 17 (UNPERTURBED)
RUN 18 (NO$_x$ SOURCE, ~ 45°N, 20 km)
RUN 19 (NO$_x$ SOURCE, ~ 45°N, 17 km)
RUN 20 (NO$_x$ SOURCE, ~ 10°N, 20 km)
TOTAL OZONE (DOBSON UNITS)
400
350
300
250
200
WINTER
SUMMER
90°N
60°N
30°N
0°
30°S
60°S
90°S
LATITUDE

Fig. 12a.

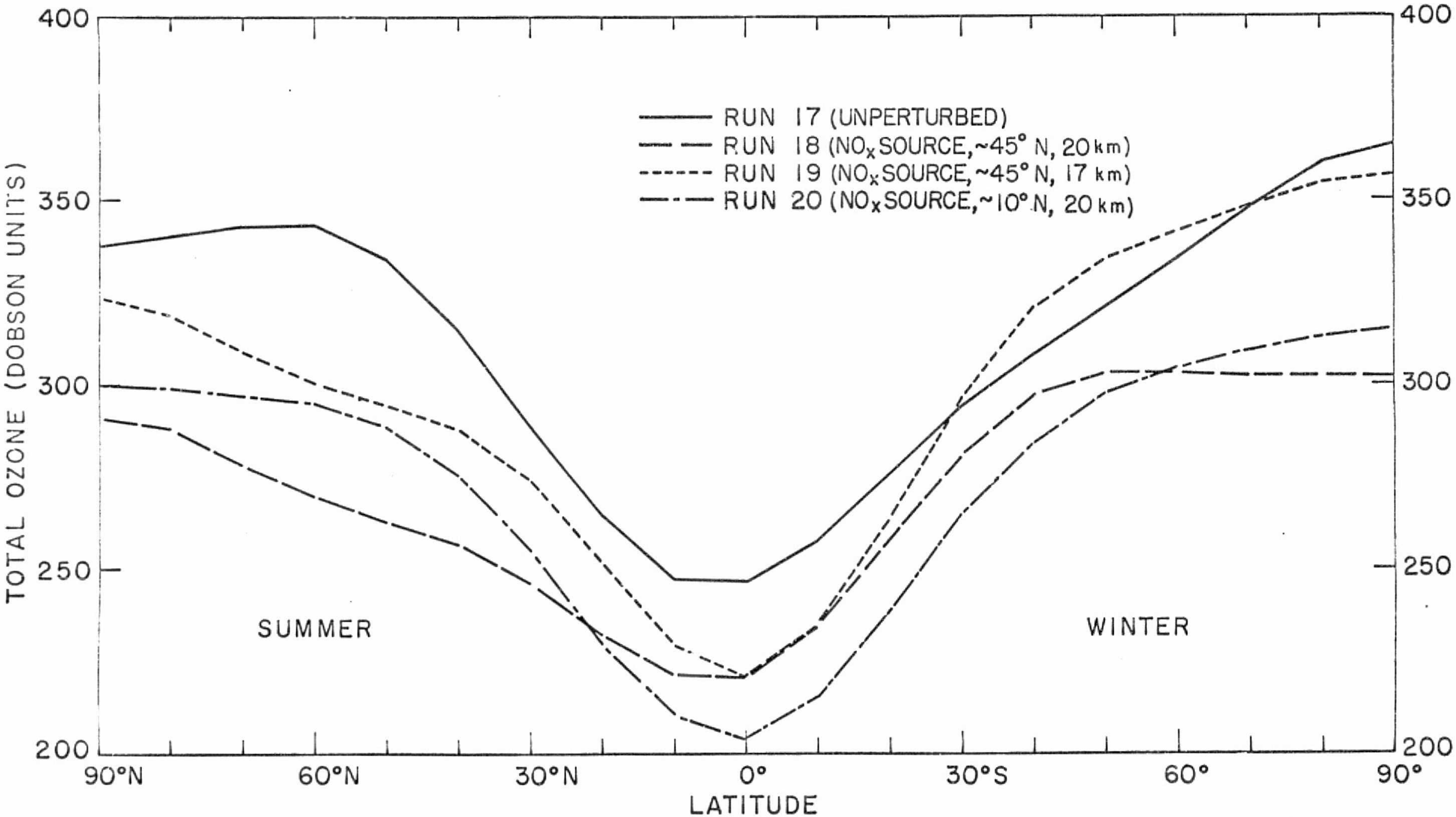
RUN 17 (UNPERTURBED)
RUN 18 (NO_x SOURCE, ~45° N, 20 km)
RUN 19 (NO_x SOURCE, ~45° N, 17 km)
RUN 20 (NO_x SOURCE, ~10° N, 20 km)
TOTAL OZONE (DOBSON UNITS)
400
350
300
250
200
SUMMER
WINTER
90°N
60°N
30°N
0°
30°S
60°
90°
LATITUDE

Figure 12b.